

Deficiency or inhibition of lysophosphatidic acid receptor 1 protects against hyperoxia-induced lung injury in neonatal rats

X. Chen,¹ F. J. Walther,^{1,2} R. van Boxtel,³ E. H. Laghmani,¹ R. M. A. Sengers,¹ G. Folkerts,⁴ M. C. DeRuiter,⁵ E. Cuppen³ and G. T. M. Wagenaar¹

¹ Division of Neonatology, Department of Pediatrics, Leiden University Medical Center, Leiden, the Netherlands

² Department of Pediatrics, Los Angeles Biomedical Research Institute at Harbor-UCLA Medical Center, Torrance, CA, USA

³ Hubrecht Institute for Developmental Biology and Stem Cell Research, Cancer Genomics Center, Royal Netherlands Academy of Sciences and University Medical Center Utrecht, Utrecht, the Netherlands

⁴ Department of Pharmacology, Utrecht Institute for Pharmaceutical Sciences, Utrecht University, Utrecht, the Netherlands

⁵ Department of Anatomy and Embryology, Leiden University Medical Center, Leiden, the Netherlands

Received 27 March 2015,
revision requested 23 September
2015,
revision received 14 October
2015,
accepted 15 October 2015
Correspondence: G. T. M.
Wagenaar, PhD, Division of
Neonatology, Department of
Pediatrics, P3-P30, Leiden
University Medical Center, PO
Box 9600, 2300 RC Leiden, the
Netherlands.
E-mail: g.t.m.wagenaar@lumc.nl

Abstract

Aim: Blocking of lysophosphatidic acid (LPA) receptor (LPAR) 1 may be a novel therapeutic option for bronchopulmonary dysplasia (BPD) by preventing the LPAR1-mediated adverse effects of its ligand (LPA), consisting of lung inflammation, pulmonary arterial hypertension (PAH) and fibrosis.

Methods: In Wistar rats with experimental BPD, induced by continuous exposure to 100% oxygen for 10 days, we determined the beneficial effects of LPAR1 deficiency in neonatal rats with a missense mutation in cytoplasmic helix 8 of LPAR1 and of LPAR1 and -3 blocking with Ki16425. Parameters investigated included survival, lung and heart histopathology, fibrin and collagen deposition, vascular leakage and differential mRNA expression in the lungs of key genes involved in LPA signalling and BPD pathogenesis.

Results: LPAR1-mutant rats were protected against experimental BPD and mortality with reduced alveolar septal thickness, lung inflammation (reduced influx of macrophages and neutrophils, and CINC1 expression) and collagen III deposition. However, LPAR1-mutant rats were not protected against alveolar enlargement, increased medial wall thickness of small arterioles, fibrin deposition and vascular alveolar leakage. Treatment of experimental BPD with Ki16425 confirmed the data observed in LPAR1-mutant rats, but did not reduce the pulmonary influx of neutrophils, CINC1 expression and mortality in rats with experimental BPD. In addition, Ki16425 treatment protected against PAH and right ventricular hypertrophy.

Conclusion: LPAR1 deficiency attenuates pulmonary injury by reducing pulmonary inflammation and fibrosis, thereby reducing mortality, but does not affect alveolar and vascular development and, unlike Ki16425 treatment, does not prevent PAH in neonatal rats with experimental BPD.

Keywords bronchopulmonary dysplasia, fibrosis, lung inflammation, lysophosphatidic acid receptor, right ventricular hypertrophy.

Premature infants at risk for neonatal chronic lung disease or bronchopulmonary dysplasia (BPD) suffer from lung damage because of lung immaturity and subsequent treatment for respiratory distress with mechanical ventilation and/or reactive oxygen species generated by (prolonged) exposure to supplemental oxygen. BPD leads to permanently enlarged alveoli, caused by an arrest in alveolar and vascular development, and a subsequent reduction in the alveolar surface and lung function (Jobe 1999, Baraldi & Filippone 2007). Serious complicating factors in the perinatal period are inflammation and oxidative stress, and at later stages pulmonary arterial hypertension (PAH)-induced right ventricular hypertrophy (RVH) and fibrosis (Baraldi & Filippone 2007, Abman 2009, Tuder *et al.* 2009, Steinhorn 2010). Similar to premature infants suffering from BPD, neonatal rats that are exposed to hyperoxia show chronic lung inflammation, persistent alveolar simplification, fibrosis, PAH and RVH (de Visser *et al.* 2010, 2012).

Lysophosphatidic acid (LPA) is a small glycerophospholipid, generated by the enzymatic removal of the choline group by extracellular autotaxin (lysophospholipase D) or phospholipase A1 or A2. LPA has a widespread tissue distribution and is secreted in the circulation (Rancoule *et al.* 2011). LPA exerts its multiple biological effects on cell proliferation, migration, survival, differentiation, motility, cytoskeletal change, inflammation and cell–cell interaction after binding to G-protein-coupled receptors (LPAR1–6) via multiple signalling pathways (Choi *et al.* 2010). LPA is involved in many pathological processes, including neurological disorders, cardiovascular disease, inflammation, lung and renal fibrosis and cancer (Choi *et al.* 2010, Lin *et al.* 2010, Pyne *et al.* 2013). Experimental and clinical evidence strongly suggests that LPA is involved in lung pathology and disease, including airway repair and remodelling, inflammation and fibrosis via LPA receptor signalling (Toews *et al.* 2002, Tager *et al.* 2008, Oikonomou *et al.* 2012, Shea & Tager 2012, Zhao & Natarajan 2013). LPAR1 or endothelial differentiation gene (EDG) family member 2 (EDG2), is the first identified LPA receptor with high affinity to LPA. In humans and rodents, LPAR1 is expressed in most organs and tissues, including the gastro-intestinal tract, heart, lung, brain, kidney, male and female reproductive organs, spleen and thymus (Choi *et al.* 2010). LPAR1 couples with three types of G proteins: *Gα12/13*, *Gαq/11*, *Gαi/o*, resulting in the initiation of several downstream signalling cascades: Rho-ROCK pathway, phospholipase C pathway, Ras-MAPK pathway, Akt pathway and adenylyl cyclase inhibition (Lin *et al.* 2010). Beneficial effects of reduced LPAR1 signalling in pulmonary disease have been demonstrated in fibroblasts of patients with idio-

pathic pulmonary fibrosis (Tager *et al.* 2008) and in rodents, as LPAR1-deficient mice are protected against fibrosis and mortality after bleomycin-induced pulmonary fibrosis (Tager *et al.* 2008) and LPS-induced lung inflammation (Zhao *et al.* 2011), and pharmacological blocking of LPAR1 protects against lung fibrosis (Swaney *et al.* 2010) and LPS-induced lung injury (Zhao *et al.* 2011). LPA is also a potent bronchoconstrictor, suggesting a role in airway hyperresponsiveness and asthma (Toews *et al.* 2002).

The role of LPAR1 deficiency in BPD remains unknown, but may result in the identification of a novel therapy with specific LPAR1 antagonists for chronic lung disease, including BPD. To advance our knowledge on LPAR1 signalling in neonatal cardiopulmonary disease *in vivo*, we studied the beneficial effects of LPAR1 blocking in neonatal rats with experimental BPD induced by prolonged exposure to hyperoxia using two different models: (i) LPAR1-mutant rats (van Boxtel *et al.* 2011) and (ii) pharmacological treatment with the LPAR1 and -3 inhibitor Ki16425 (Rancoule *et al.* 2011). We then investigated inflammation, alveolarization, fibrosis, PAH and RVH in the lung as described previously (de Visser *et al.* 2010).

Materials and methods

Animals

The research protocol was approved by the Institutional Animal Care and Use Committee of the Leiden University Medical Center and the Royal Dutch Academy of Sciences. LPAR1-mutant rats carry a missense mutation with a methionine instead of arginine at position 318 in the cytoplasmic 8th helix, resulting in a loss-of-function phenotype. This mutation was induced by an N-ethyl-N-nitrosourea (ENU)-driven target-selected mutagenesis approach in Wistar rats (van Boxtel *et al.* 2010, 2011). LPAR1-mutant rats were backcrossed for seven generations on a Wistar background. For each experiment newborn wild-type Wistar rat pups from two litters and homozygous LPAR1-mutant (LPAR1^{M318R/M318R}) newborn rat pups from two litters were pooled. Hereafter, wild-type and LPAR1^{M318R/M318R} mutant neonatal rat pups were equally distributed over the experimental groups: an oxygen group (*N* = 12) and two room air (RA)-exposed control groups (*N* = 6). All pups were fed by wild-type Wistar foster dams. For the intervention experiments neonatal rat pups were pooled and distributed over four experimental groups (*N* = 6): an oxygen-DMSO, oxygen-Ki16425, RA-DMSO and RA-Ki16425 group injected either with DMSO or Ki16425. The oxygen concentration, body weight, evi-

dence of disease and mortality were monitored daily. Adult Wistar rats (6 months old; $N = 5$) were exsanguinated after induction of anaesthesia with an intraperitoneal injection of ketamine (50 mg kg^{-1}) and xylazine (50 mg kg^{-1}). Lungs were stored at -80°C until isolation of RNA for *real-time* RT-PCR and hearts were fixed in formalin. On neonatal days 7 and 15 the thorax was opened under anaesthesia to visualize the ductus arteriosus in wild-type and LPAR1^{M318R/M318R} mutant neonatal rat pups *in situ* ($N = 2$). Hereafter, hearts were removed, fixed in formalin and processed for histology.

Hyperoxia-induced neonatal lung injury

Pups (a mix of both sexes) were continuously exposed to 100% oxygen for 10 days. In the intervention experiments pups received from day 2 either $5 \text{ mg kg}^{-1} \text{ day}^{-1}$ Ki16425 (Selleckchem S1315; Bioconnect, Huizen, the Netherlands) or DMSO (10%) in 0.9% NaCl ($100 \mu\text{L}$, subcutaneously). Lung and heart tissue were collected on day 10 under anaesthesia. Separate experiments were performed for (i) histology, (ii) frozen lung tissue and (iii) collection of bronchoalveolar lavage fluid (BALF). Lungs were snap-frozen in liquid nitrogen for *real-time* RT-PCR and fibrin deposition assay or fixed in formalin for histology studies as previously described (de Visser *et al.* 2009).

Primary rat embryonic fibroblast isolation

Embryonic fibroblasts, known to express LPAR1 (Stortelers *et al.* 2008), were used to functionally characterize the molecular consequences of the LPAR1 mutation. Heterozygous LPAR1-mutant rats were mated and at day 13.5 embryos were isolated. After washing the embryo thoroughly, the head and visceral organs were removed and used for DNA isolation and genotyping by PCR and sequencing using the following primer set: forward primer: 5'-AGATCCTCT-CAGGCTGGTC-3' and reverse primer (5'-ACAGGA GTGTCTTCGTCTCC-3') as described previously (van Boxel *et al.* 2010). The embryos were minced and treated with trypsin to get a single cell suspension. Adherent rat embryonic fibroblasts (REFs) were grown in DMEM supplemented with 10% FCS.

In vitro fusion protein expression studies

Wild-type and mutant receptors were N-terminally haemagglutinin (HA)-tagged by cloning into the expression vector pcDNA3.1 (Invitrogen, Life Technologies, Carlsbad, CA, USA). The receptor fusion protein constructs were transfected with a similar efficiency for both HA-tagged wild-type and mutant

LPAR1 plasmids and expressed in COS-7 cells (Figure S1). COS-7 cells were seeded on a coverslip and 24 h after transfection the cells were placed on ice and incubated with DMEM-buffered HEPES containing 0.2% fatty acid-free bovine serum albumin (DHB) for 15 min. Subsequently, the cells were incubated for 1 h with a polyclonal rabbit anti-HA (ab137838; Abcam, Cambridge, UK) on ice in DHB at a 1 : 500 dilution. For cell surface expression analysis the cells were immediately methanol-fixed and washed thoroughly with PBS and incubated for one hour in blocking buffer (1% BSA in 0.1% PBS-Tween) at room temperature. The cells were washed three times with PBS and incubated for 1 h with a secondary anti-rabbit antibody conjugated with FITC (ab97050; Abcam), diluted 1 : 500 at room temperature in the dark. After three times washing with PBS the coverslips were mounted using Vectashield with DAPI (Brunschwig chemie, Amsterdam, the Netherlands) and analysed using confocal microscopy. For western blotting COS-7 cells were lysed 24 h after transfection, the proteins were separated on a SDS gel (10% acrylamide gradient; Bio-Rad, Veenendaal, the Netherlands) and transferred to a nitrocellulose membrane. The membrane was incubated for 1 h at room temperature with a 1 : 500 or 1 : 1000 dilution of, respectively, a polyclonal rabbit anti-HA antibody (ab13834; Abcam) or a polyclonal rabbit anti-actin antibody (A2066; Sigma-Aldrich, St. Louis, MO, USA) in blocking buffer followed by an incubation for 1 h with peroxidase-conjugated, anti-rabbit IgG diluted 1 : 5000 in blocking buffer at room temperature. Protein bands were detected by using the enhanced chemiluminescence detection method (ECL; Amersham Biosciences/GE Healthcare, Eindhoven, the Netherlands).

Cell surface ELISA

Surface expression of N-terminally HA-tagged receptors was quantified as described (Gehret *et al.* 2010). Briefly, the N-terminally tagged receptors were transiently expressed in COS-7 cells and 24 h after transfection the cells were harvested, seeded in 12-well plates and serum-starved overnight. To specifically measure the pool of cell surface-expressed receptors, the cells were placed on ice and incubated with DMEM-buffered HEPES containing 0.2% fatty acid-free bovine serum albumin (DHB) for 15 min. Subsequently, the cells were incubated for 1 h with a polyclonal rabbit anti-HA (ab137838; Abcam) on ice in DHB at a 1 : 500 dilution, rinsed with PBS on ice, fixed with ice-cold methanol : acetone (1 : 1) and air-dried. Cells were then washed 5 min with PBS, blocked with RIPA/milk buffer (150 mM NaCl,

50 mM Tris, 1 mM EDTA, 10 mM NaF, 100 nM sodium orthovanadate, 1% Triton X-100, 0.1% SDS, 0.5% sodium deoxycholate, pH 8.0 and 5% non-fat dried milk). To measure the total pool of N-terminally tagged receptors, cells were first fixed with ice-cold methanol : acetone (1 : 1), air-dried and then washed 5 min with PBS. Subsequently, the cells were blocked with RIPA/milk buffer and incubated with 1 : 500 anti-HA antibody (ab13834; Abcam). All cells were then washed three times 5 min with PBS and incubated with peroxidase-conjugated, anti-rabbit IgG diluted 1 : 5000 in RIPA/milk buffer. The cells were washed three times 5 min with PBS and incubated with ELISA TMB reagent (Sigma-Aldrich). The reaction was terminated with stop reagent for TMB substrate (Sigma-Aldrich) and the absorbance was measured at 450 nm. Data were presented as the A_{450} of the pool of cell surface-expressed receptors as a percentage of the A_{450} of the total pool of HA-tagged receptors.

ERK1/2 phosphorylation analysis

Primary REFs were seeded in 12-wells plates and allowed to attach overnight. Subsequently, the cells were serum-starved overnight in DMEM supplemented with 0.2% fatty acid-free BSA, and with or without the presence of 100 ng mL⁻¹ pertussis toxin (PTX). Cells were treated with 1 mM LPA and lysed with RIPA buffer supplemented with complete protease inhibitor cocktail (Roche Diagnostics, Woerden, the Netherlands) and PhosSTOP phosphatase Inhibitor Cocktail (Roche Diagnostics) at the indicated time points. Western blot analysis was performed as described above with a mouse antibody against pT183 and pY185 in human ERK1 and ERK2 (ab50011; Abcam; diluted 1 : 5000) and a rabbit antibody against total rat ERK1 and ERK2 (91021; Cell Signaling Technology, Danvers, MA, USA; diluted 1 : 1000).

Histology

Formalin-fixed, paraffin-embedded, 4- μ m-thick heart and lung sections were stained with haematoxylin and eosin or Hart's stained to visualize elastin (Simon *et al.* 2010). Lungs were immunostained additionally with anti-LPAR1 (AP01253PU-N or SP4371P; Acris antibodies, San Diego, CA, USA, diluted 1 : 1000), anti-ED-1 (monocytes and macrophages; 1 : 5), anti-myeloperoxidase (MPO, RB-373-A1; Thermo Fisher Scientific, Fremont, CA, USA; diluted 1 : 1500), anti- α smooth muscle actin (ASMA, A2547, Sigma-Aldrich; diluted 1 : 20 000), anti-collagen III (COL3A1, ab7778; Abcam; diluted 1 : 3000) or anti-von Willebrand factor (vWF, A0082; Dako Cytomation,

Glostrup, Denmark; diluted 1 : 4000) using standard methods (de Visser *et al.* 2009). Quantitative morphometry was performed by two independent researchers blinded to the treatment strategy as previously described (Yi *et al.* 2004, de Visser *et al.* 2009, Wagenaar *et al.* 2013).

Fibrin detection assay

Quantitative fibrin deposition in lung tissue homogenates was determined by Western blotting as described previously (de Visser *et al.* 2009, Wagenaar *et al.* 2013). Tissue samples were dissolved in reducing sample buffer (10 mM Tris pH 7.5, 2% SDS, 5% glycerol, 5% -mercaptoethanol and 0.4 mg mL⁻¹ of bromophenol blue), subjected to SDS-PAGE (7.5% gel; 5% stacking gel) and blotted onto PVDF membrane (Immobilon-FL; Millipore, Bedford, MA, USA). The 56-kDa fibrin β -chains were detected with monoclonal 59D8 (Oklahoma Medical Research Foundation, Oklahoma City, OK, USA; diluted 1 : 1000), infrared-labelled goat-anti-mouse secondary antibody (IRDye 800CW; Licor Biosciences, Lincoln, NE, USA, diluted 1 : 5000) and quantified using an infrared detection system (Odyssey infrared imaging system; Licor Biosciences, Lincoln, NE, USA). Fibrin deposition was quantified using rat fibrin as a reference.

Bronchoalveolar lavages, protein assay and CINC1 ELISA

Lung lavages, protein and CINC1 ELISA (ADI-900-074, Enzo Life Sciences, Raamsdonksveer, the Netherlands) were performed as previously described (de Visser *et al.* 2009, Wagenaar *et al.* 2013).

Real-time RT-PCR

Total RNA isolation from lung tissue homogenates (RNA-Bee; Tel-Test, Bio-Connect BV, Huissen, the Netherlands), first-strand cDNA synthesis [SuperScript Choice System (Life Technologies, Breda, the Netherlands)] and *real-time* quantitative PCR, using β -actin as a housekeeping gene reference, were performed on a LightCycler 480 (Roche, Almere, the Netherlands) of the Leiden Genome Technology Center (Leiden, the Netherlands) as described previously (Wagenaar *et al.* 2004, 2013). Primers are listed in Table 1.

Statistical analysis

Values are expressed as mean \pm SEM. Differences between groups were analysed with ANOVA, followed by Tukey's multiple comparison test. Differences at P -values < 0.05 were considered statistically significant.

Table 1 Sequences of oligonucleotides for forward and reverse primers for real-time RT-PCR

Gene product	Forward primer	Reverse primer
CINC1	5'-GCACCCAAACCGAAGTCATA-3'	5'-GGGGACACCCTTTAGCATCT-3'
LPAR1	5'-TGTGCTGGGTGCCTTTATTG-3'	5'-GGCAACACACATCGAGCAGTA-3'
LPAR2	5'-CACTGCCTCTGTGACTTGGA-3'	5'-AGACAAGCAGGCTGGATAGG 3'
LPAR3	5'-ACACGAGTGGCTCCATCAG-3'	5'-CCACGAAGGCTCCTAAGACA-3'
LPAR4	5'-ACCATCAGGACCAGGAGGAAT-3'	5'-CCACTGAGGACTAGGATCCAGACT-3'
LPAR5	5'-TCCTACTGGCCAACCTCATC-3'	5'-GGCCTGAAGGCTGTTCTTTA-3'
LPAR6	5'-CTCTGCATTGCTGTCTCCAA-3'	5'-TGAGTTCTGGATCGTGTCTGA-3'
MCP1	5'-ATGCAGTTAATGCCCCAGTCA-3'	5'-TTCTCCAGCCGACTCATTGG-3'
PAI-1	5'-AGCTGGGCATGACTGACATCT-3'	5'-GCTGCTCTTGGTCGGAAAAGA-3'
TF	5'-CCCAGAAAGCATCACCAAGTG-3'	5'-TGCTCCACAATGATGAGTGT-3'
β -actin	5'-TTCAACACCCAGCCATGT-3'	5'-AGTGGTACGACCAGAGGCATACA-3'

TF, tissue factor.

Results

Dose finding for Ki16425 in experimental BPD

To determine the optimal dosing of Ki16425, we performed a pilot experiment in which hyperoxia-exposed rat pups were treated with 1–5 mg kg⁻¹ day⁻¹ Ki16425 or DMSO (2–10% in 0.9% NaCl. Ki16425 has anti-inflammatory properties (Zhao *et al.* 2011) and preliminary data with the LPAR1-deficient animals showed a reduced influx of macrophages in mutant rat pups with experimental BPD compared to wild-type controls. Therefore, we used the influx of macrophages to the lung as a read-out and demonstrated that 5 mg kg⁻¹ day⁻¹ of Ki16425 was the most optimal dose to reduce the influx of macrophages into the lung in hyperoxia-induced BPD (Fig. 1).

Effects of LPAR1^{M318R} mutation on LPAR1 expression in the lung

In the neonatal rat lung on day 10 highest LPAR1 protein expression was observed in the bronchial epithelial layer (Fig. 2a). In addition, protein expression was observed in alveolar type 2 cells and in arterioles in the endothelium and vascular smooth muscle cells, and in inflammatory cells. A similar pattern of expression was observed after exposure to hyperoxia (Fig. 2b) and in LPAR1-deficient rat pups under normoxia (Fig. 2c) and hyperoxia (Fig. 2d).

LPAR1^{M318R} results in a hypomorphic phenotype in rats

Using N-ethyl-N-nitrosourea (ENU)-driven target-selected mutagenesis, a mutation was identified in LPAR1 that resulted in the substitution of methionine 318 into an arginine in the putative helix 8 of the receptor (Fig. 3a; van Boxtel *et al.* 2011). The hydrophobic-

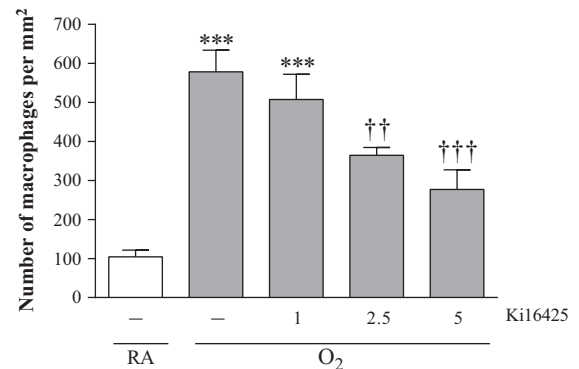


Figure 1 Pilot experiment to find the optimal dose of Ki16425 for treatment of experimental bronchopulmonary dysplasia (BPD) by determining the pulmonary influx of ED-1-positive monocytes and macrophages in tissue sections in room air (RA), pups injected daily with DMSO (10%, open bar) and O₂-exposed pups (O₂) injected daily with 10% DMSO or Ki16425 (shaded bars): 1, 2.5 and 5 mg kg⁻¹ day⁻¹. Data are expressed as mean ± SEM. ****P* < 0.001 vs. RA control. ††*P* < 0.01 and †††*P* < 0.001 vs. age-matched DMSO-treated O₂-exposed control; *n* = 4–8 per group.

ity of the affected residue is highly conserved in the GPCR class A family. Furthermore, this position is analogous to the phenylalanine of the NPxxY(x)5,6F motif found in many GPCRs, including the prototypic Rhodopsin and β 2 adrenergic receptor (ADRB2; Fig. 3a). The residue sticks into a hydrophobic pocket and contacts the tyrosine of the same motif, which is important for the folding of the 8th helix. Computational analyses suggest that the amino acid change in the LPAR1 mutant will disrupt this hydrophobic interaction and additionally, an arginine is too big to fit in this pocket and will most probably result in incorrect packing of helix 8 (van Boxtel *et al.* 2011). In line with this, LPAR1-mutant rats showed a craniofacial malfor-

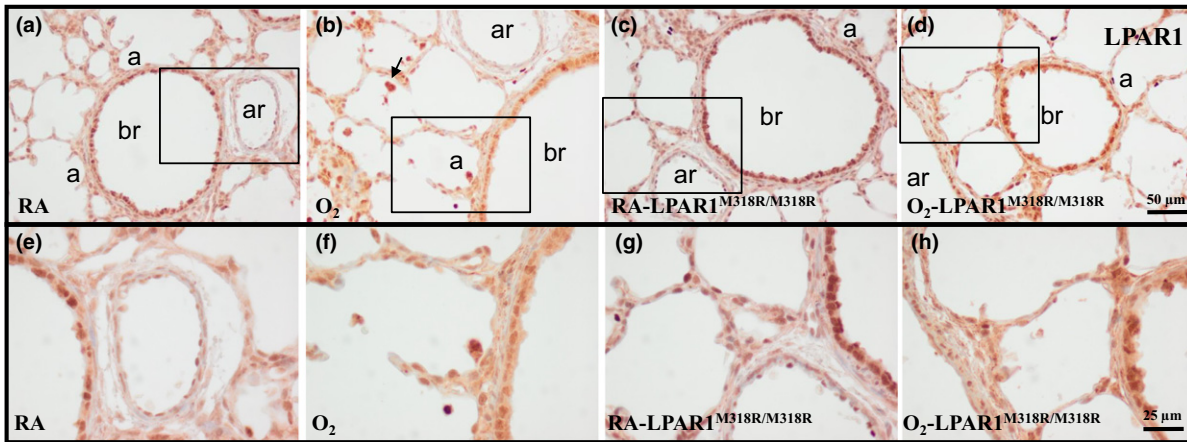


Figure 2 Representative lung sections stained for lysophosphatidic acid receptor 1 [LPAR1 or endothelial differentiation gene 2 (EDG2); a–h] of wild-type (a, b, e and f) and LPAR1-mutant rat pups (c, d, g and h) kept in room air (RA; a, c, e and g) or 100% O₂ (b, d, f and h) until 10 days of age. Boxed areas in panels (a), (b), (c) and (d) are represented in panels (e), (f), (g) and (h) respectively. a, alveolus; ar, arteriole; br, bronchus. Arrow in panel (b) indicates LPAR1-positive inflammatory cells.

mation with an increase in the distance between both eyes and a shortening of the eye to nose tip distance (Fig. 3b; van Boxtel *et al.* 2011), similarly as observed in LPAR1 knockout mice (Contos *et al.* 2000).

To test the molecular effect of the mutation on LPAR1 function, we first tested if LPAR1^{M318R} could still be transported and expressed in the plasma membrane, the site of action of the receptor. Although membrane expression was still observed in cells overexpressing mutant LPAR1 (LPAR1^{M318R}), it was considerably less compared to wild-type receptor (Fig. 3c). Interestingly, cell surface-expressed mutant LPAR1 displayed a punctate appearance (Fig. 3c), which can be indicative for receptor clustering in clathrin-coated pits and aberrant internalization of mutant LPAR1. Western blot analysis of lysates of cells overexpressing LPAR1 revealed a slightly decreased expression level of mutant compared to wild-type receptor (Fig. 3d), which could reflect receptor instability or degradation. Therefore, we quantified cell membrane expression using a cell surface ELISA and indeed observed that the pool of cell surface-expressed HA-LPAR1^{M318R} as a percentage of the total expressed mutant receptor was significantly decreased compared to HA-LPAR1^{WT} (Fig. 3e). One of the pathways activated by LPA is the mitogen-activated protein (MAP) kinase cascade via pertussis toxin (PTX)-sensitive G_i in a tyrosine kinase-dependent manner (Moolenaar *et al.* 2004). This pathway is thought to be the main mediator of the stimulatory effect of LPA on cell proliferation. To test the effect of LPAR1^{M318R} on the LPA-induced MAP kinase-signalling cascade, we isolated primary REFs that endogenously express LPAR1 and tested activation of the MAP kinase-signalling cascade in these cells. For

this, serum-starved homozygous mutant and wild-type REFs were stimulated with LPA and ERK1/2 phosphorylation was measured. LPA treatment resulted in a rapid and transient ERK1/2 phosphorylation response (Fig. 3f). In contrast, homozygous mutant REFs show an attenuated LPA-induced ERK1/2 phosphorylation response, demonstrating that M318R in LPAR1 diminishes LPA signalling in primary REFs. These results demonstrate that the LPAR1^{M318R} mutation results in a hypomorphic phenotype in rats.

Effects of LPAR1^{M318R} mutation and Ki16425 treatment on bodyweight and survival

On day 10, body weight was comparable in Wistar control and LPAR1-mutant rats kept in RA (19–20 g; Fig. 4a) and in 100% oxygen (12 g). Administration of Ki16425 or its solvent DMSO to Wistar control rats for 10 days had no adverse effects on mean body weight in RA controls and oxygen-exposed pups. Exposure to hyperoxia resulted in a 40% survival on day 10 in non-treated and 60% in DMSO-treated Wistar rats and was not affected by administration of Ki16425 (Fig. 4b). In LPAR1-mutant rats with experimental BPD survival was twofold higher than in non-treated O₂-exposed Wistar control rats (80%, $P < 0.05$). RA-exposed pups showed no morbidity or mortality during the experimental period of 10 days.

Effects of LPAR1^{M318R} mutation and Ki16425 treatment on lung airway development and inflammation

Ten days after birth, LPAR1 deficiency or administration of Ki16425 or DMSO did not have adverse effects in the lung (Fig. 5) on the number of alveolar

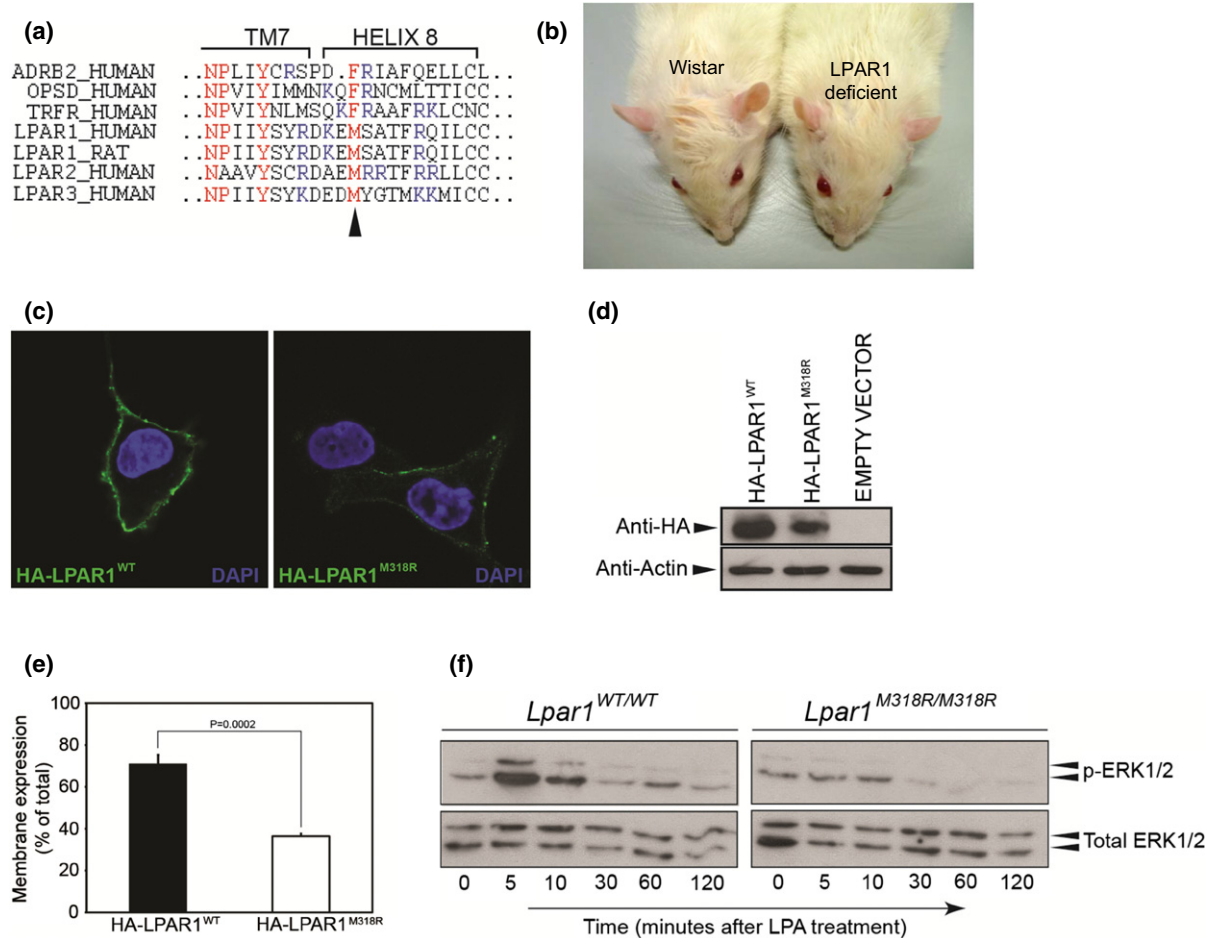


Figure 3 Non-synonymous mutation in the LPAR1 gene results in a hypomorphic phenotype. (a) Alignment of amino acid sequence of the 8th helices of different class A GPCRs. Indicated in red is the NPxxY(x)_{5,6}F motif of which the tyrosine in transmembrane (TM) 7 domain and the phenylalanine in helix 8 form a hydrophobic interaction in the inactive state. In LPAR1–3 the phenylalanine is replaced by a methionine, conserving hydrophobicity. The arrowhead indicates the location of the amino acid change caused by the mutation. Indicated in blue are the basic amino acids that are commonly found in helix 8. (b) LPAR1-mutant rats have a craniofacial malformation with a shortening of the eye to nose tip distance and an increase in the distance between the eyes compared to wild-type Wistar rats. (c) Decreased membrane expression of overexpressed LPAR1^{M318R} compared to overexpressed wild-type receptor. Intact serum-starved COS-7 cells expressing N-terminally haemagglutinin (HA)-tagged wild-type or mutant LPAR1 were incubated with an anti-HA antibody. The antibody can only bind if the cell expresses the receptor in the membrane, because only then the HA-tag is localized outside the cell. (d) Western blot analysis of COS-7 cells overexpressing either HA-LPAR1^{WT} or HA-LPAR1^{M318R}. (e) The size of the cell surface-expressed receptor pool as percentage of the total receptor pool is decreased in cells expressing LPAR1^{M318R}. Graph indicates the pool of cell surface-expressed receptor as a percentage of total HA-tagged-expressed receptors measured by cell surface ELISA. (f) LPAR1^{M318R/M318R} rat embryonic fibroblasts (REFs) display a hypomorphic ERK1/2 phosphorylation pattern. Western blot analysis of MAP kinase pathway activation in wild-type and mutant REFs after 1 mM LPA treatment.

crests (Fig. 6a), pulmonary vessel density (Fig. 6b), arterial medial wall thickness (Fig. 6c), alveolar septal thickness (Fig. 6d), and influx of macrophages (Fig. 6e) and neutrophilic granulocytes (Fig. 6f). Oxygen exposure for 10 days resulted in lung oedema, a heterogeneous distribution of enlarged air-spaces (Fig. 5b) with a decreased number of alveolar crests (2.4-fold, $P < 0.001$; Fig. 6a) surrounded by septa with increased thickness (1.9-fold, $P < 0.001$; Figs 5b and 6d), reduced pulmonary vessel density (2.1-fold,

$P < 0.001$; Figs 5b and 6b) and increased pulmonary arterial medial wall thickness (2.4-fold, $P < 0.001$; Figs 5f and 6c). Exposure to hyperoxia also led to an inflammatory response, characterized by an overwhelming influx of macrophages (6.7-fold, $P < 0.001$ in LPAR1-deficient rats and 6.0-fold, $P < 0.001$ in Ki16425-treated rats, Figs 5j and 6e) and neutrophils (5.7-fold, $P < 0.01$ in LPAR1-deficient experiments and 4.5-fold, $P < 0.001$ in Ki16425 experiments, Figs 5n and 6f), compared to RA-exposed controls.

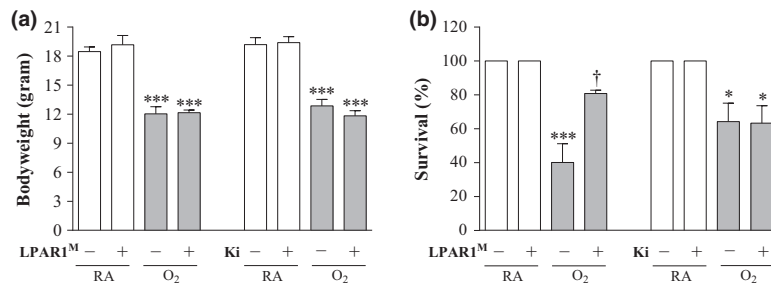


Figure 4 Growth (a) and survival (b) on day 10 in room air (RA) and age-matched O₂-exposed wild-type or LPAR1-mutant rat pups (O₂). Wild-type Wistar rats were injected daily with DMSO (10%) or Ki16425 (5 mg kg⁻¹ day⁻¹) for 10 days. Open bars: RA and RA-LPAR1-mutant or Ki16425-treated pups, shaded bars: O₂-control, O₂-LPAR1 mutant or O₂-Ki16425 treatment. Data are expressed as mean ± SEM. **P* < 0.05 and ****P* < 0.001 vs. own RA controls. †*P* < 0.05 vs. age-matched O₂-exposed control. LPAR1^M = LPAR1^{M318R/M318R}-mutant rat; Ki = Ki16425. -: daily administration of solvent (DMSO) in Ki16425 experiments or wild-type rat in LPAR1-mutant rat experiments. +: daily treatment with 5 mg kg⁻¹ of Ki16425 or LPAR1-mutant rat in 4–7 independent experiments per group.

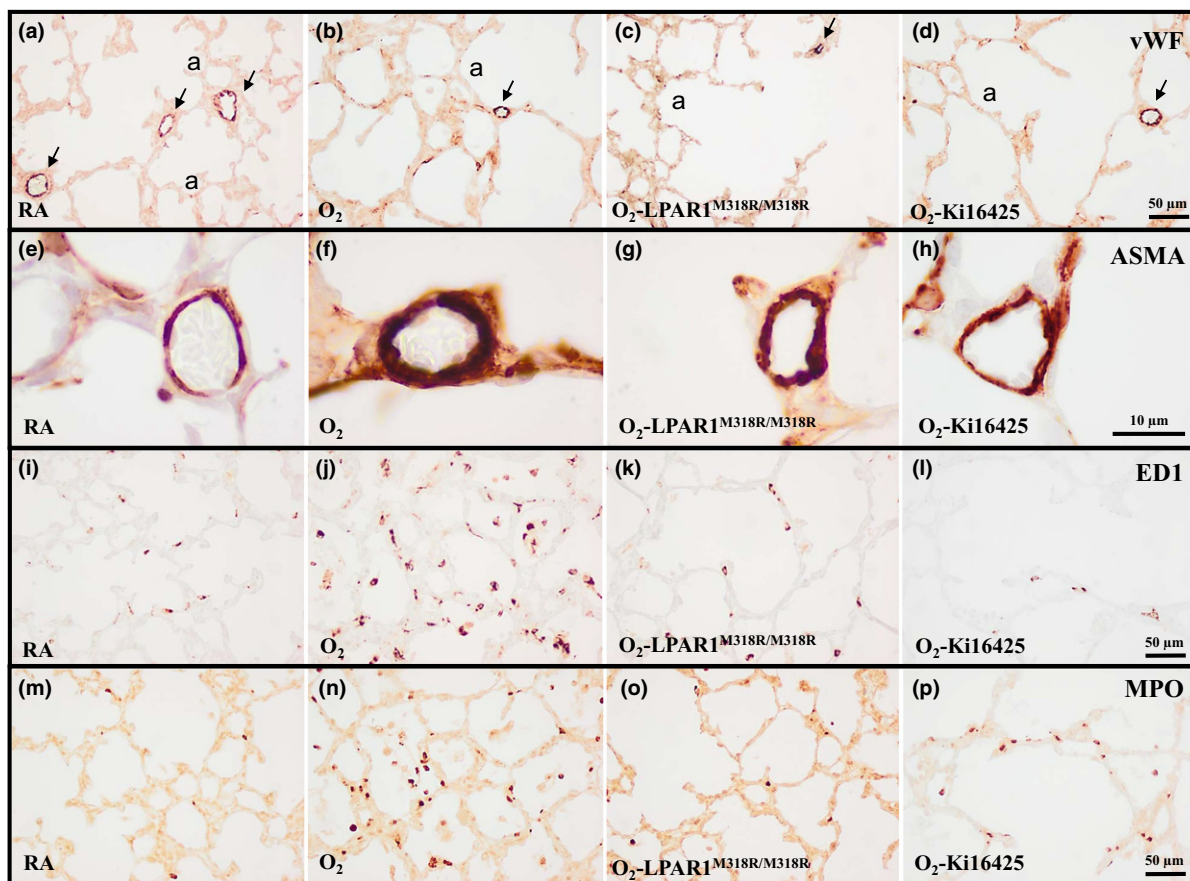


Figure 5 Representative lung sections stained for von Willebrand Factor (vWF; a–d), α smooth muscle actin (ASMA; e–h), the monocyte and macrophage marker ED1 (i–l) or myeloperoxidase (MPO) as a marker for neutrophilic granulocytes (m–p) of wild-type (a, b, d–f, h–j, l–n and p) and LPAR1-mutant rat pups (c, g, k and o) kept in room air (RA; a, e, i and m) or 100% O₂ (b–d, f–h, j–l and n–p) injected daily with 10% DMSO (a, b, e, f, i, j, m and n) or 5 mg kg⁻¹ day⁻¹ of Ki16425 (d, h, l and p) until 10 days of age. a, alveolus. Arrows in panels (a–d) indicate vWF-positive blood vessels.

In LPAR1-deficient rat pups reduced alveolar septal thickness (1.4-fold, *P* < 0.001; Figs 5c and 6d) and influx of macrophages (2.2-fold, *P* < 0.01; Figs 5k

and 6e) and neutrophils (3.8-fold, *P* < 0.01; Figs 5o and 6f) were observed compared to oxygen-exposed controls, but beneficial effects on hyperoxia-induced

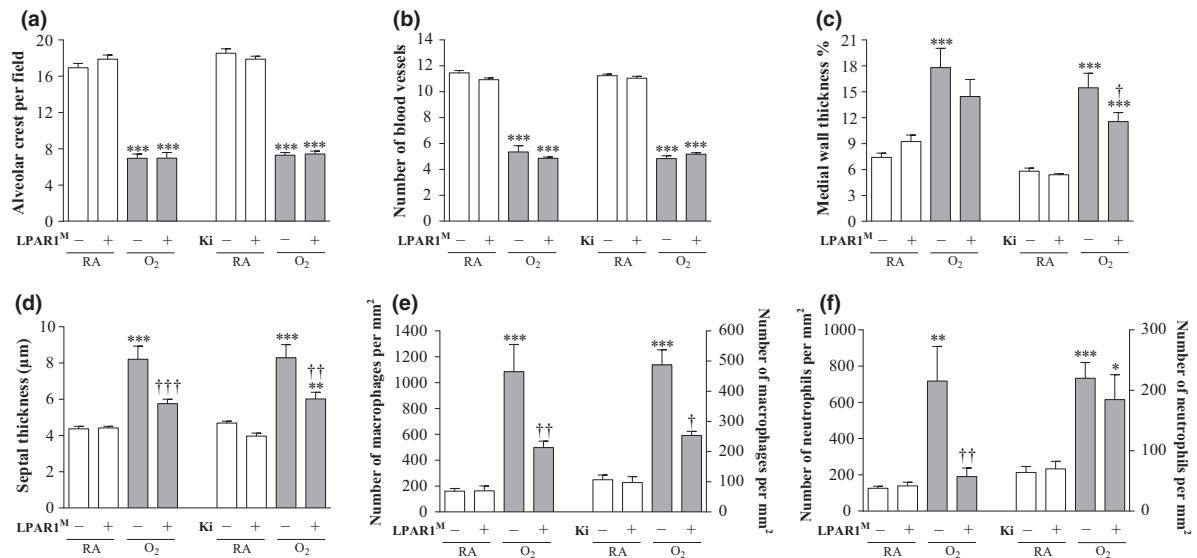


Figure 6 Lung morphometry, including the quantifications of alveolar crests (a), number of pulmonary vessels (b), arterial medial wall thickness (c), septal thickness (d) and influx of macrophages (e) and neutrophilic granulocytes (f) was determined on paraffin sections in LPAR1-mutant and wild-type Wistar rats on day 10. In the LPAR1 experiments pups did not receive treatment. Wild-type pups served as controls in room air (RA) (open bar) and hyperoxia (shaded bar) for LPAR1-mutant rat pups kept in RA (open bar) or hyperoxia (shaded bar). In the Ki16425 experiments, RA pups were injected daily with DMSO or Ki16425 (open bars) and O₂ pups were injected daily with DMSO or Ki16425 (shaded bars): 5 mg kg⁻¹ day⁻¹ until 10 days of age. Values are expressed as mean ± SEM. **P* < 0.05, ***P* < 0.01 and ****P* < 0.001 vs. own RA controls. †*P* < 0.05, ††*P* < 0.01 and †††*P* < 0.001 vs. age-matched O₂-exposed controls. LPAR1^M = LPAR1^{M318R/M318R}-mutant rat; Ki = Ki16425. –: daily administration of solvent (DMSO) in Ki16425 experiments or wild-type rat in LPAR1-mutant rat experiments. +: daily treatment with 5 mg kg⁻¹ of Ki16425 or LPAR1-mutant rat, *n* = 6–10 per group. Two independent experiments were performed with LPAR1-mutant rats and three for the Ki16425 intervention studies.

inhibition of alveolarization and angiogenesis, and increased arterial medial wall thickness were absent. Administration of Ki16425 reduced medial wall thickness 1.3-fold (*P* < 0.05; Figs 5h and 6c), alveolar septal thickness (1.4-fold, *P* < 0.01; Figs 5d and 6d) and the influx of macrophages (2.3-fold, *P* < 0.01; Figs 5l and 6e) compared to oxygen-exposed controls. Ki16425 had no beneficial effects on hyperoxia-induced inhibition of alveolarization and angiogenesis, nor on the influx of neutrophils.

Effects of LPAR1^{M318R} mutation and Ki16425 treatment on lung collagen deposition and elastin expression

In all rat pups kept under normoxia collagen III was only present at high levels in the perivasculture of large and small blood vessels (Fig. 7a). Expression was low or absent in alveolar septa. In lungs of pups exposed to hyperoxia for 10 days, collagen III deposition increased [7.3-fold, *P* < 0.001; LPAR1 experiment and 7.8-fold, *P* < 0.001; Ki16425 experiment (Fig. 7m)], and was present in the perivasculture of blood vessels and in thick alveolar septa (Fig. 7b). LPAR1 deficiency or treatment of experimental BPD with Ki16425 for 10 days reduced collagen III expression by 55% (*P* < 0.001; Fig. 7m) in the thin alveolar septa (Fig. 7c,

d). In all rat pups kept under normoxia, elastin was predominantly present on the septal tips in the alveoli and in the wall of blood vessels (Fig. 7e,f,i,j). Under normoxia, elastin expression increased 1.4-fold (*P* < 0.05; Fig. 7n) in LPAR1-deficient rats compared to Wistar controls, which can be explained by an increase in elastin expression in the small arterioles (Fig. 7f). In Wistar rats kept under hyperoxia, elastin expression decreased 1.4-fold compared to normoxia-exposed controls after DMSO administration (*P* < 0.01; Fig. 7n), and was predominantly present in the alveolar walls rather than on septal tips and in the walls of small blood vessels (Fig. 7g,k). LPAR1-deficient rats showed a 1.8-fold decrease in elastin expression after exposure to hyperoxia (*P* < 0.001; Fig. 7n). LPAR1 deficiency or treatment with Ki16425 for 10 days had no effect on elastin expression in blood vessels and on the hyperoxia-induced irregular elastin expression in alveolar walls in pups with hyperoxia-induced lung injury (Fig. 7h,l).

Effects of LPAR1^{M318R} mutation and Ki16425 treatment on coagulation, vascular leakage and CINC1 expression in BALF

Pulmonary fibrin deposition was studied in homogenates as a read-out for lung damage (Fig. 8a). Fibrin

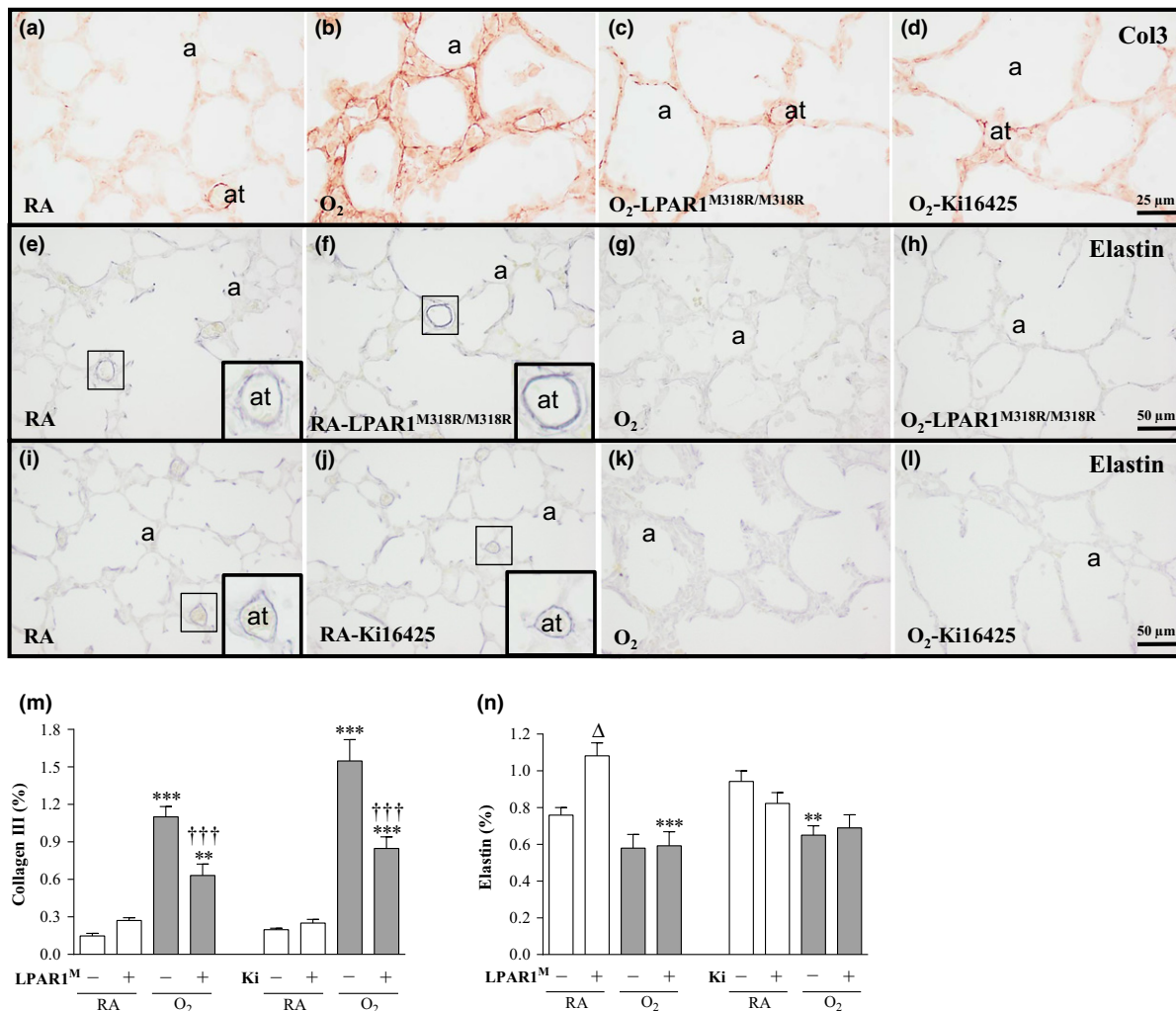


Figure 7 Representative lung sections stained for collagen III (a–d) and elastin (e–l) of wild-type (a, b, d, e, g, i–l) and LPAR1-mutant rat pups (c, f and h) kept in room air (RA; a, e, f, i and j) or 100% O₂ (b–d, g, h, k and l) injected daily with 10% DMSO (a, b, i and k) or 5 mg kg⁻¹ day⁻¹ of Ki16425 (d, j and l) until 10 days of age. Quantification of collagen III deposition (m) and elastin expression (n) on lung tissue paraffin sections on day 10 in LPAR1-mutant and wild-type Wistar rat pups. In the LPAR1 experiments pups did not receive treatment. Wild-type pups served as controls in RA (open bar) and hyperoxia (shaded bar) for LPAR1-mutant rat pups kept in RA (open bar) or hyperoxia (shaded bar). In the Ki16425 experiments, RA pups were injected daily with DMSO or Ki16425 (open bars) and O₂ pups were injected daily with DMSO or Ki16425 (shaded bars): 5 mg kg⁻¹ day⁻¹ until 10 days of age. Values are expressed as mean ± SEM. ****P* < 0.001 vs. own RA controls. ^Δ*P* < 0.05 vs. RA Wistar control. ^{†††}*P* < 0.001 vs. age-matched O₂-exposed control. LPAR1^M = LPAR1^{M318R/M318R}-mutant rat; Ki = Ki16425. -: daily administration of solvent (DMSO) in Ki16425 experiments or wild-type rat in LPAR1-mutant rat experiments. +: daily treatment with 5 mg kg⁻¹ of Ki16425 or LPAR1-mutant rat, *n* = 6–10 per group. Two independent experiments were performed with LPAR1-mutant rats and three for the Ki16425 intervention studies. a, alveolus; at, arteriole.

deposition was at reference levels in all rat pups kept under normoxia for 10 days (<20 ng fibrin mg⁻¹ tissue), and increased (29-fold, *P* < 0.01 in LPAR1 experiment and fivefold, *P* < 0.01 in Ki16425 experiment) in lungs of pups exposed to 100% oxygen for 10 days. LPAR1 deficiency or Ki16425 administration did not reduce hyperoxia-induced fibrin deposition. Total protein concentration in BALF was determined to establish the effect of pulmonary oedema by capillary-alveolar leakage (Fig. 8b). After exposure to

hyperoxia for 10 days the protein concentration increased (19-fold, *P* < 0.01; LPAR1 experiment and 11-fold, *P* < 0.05; Ki16425 experiment) and was not affected significantly in LPAR1-deficient or Ki16425-treated rat pups with experimental BPD, although Ki16425-treated pups with experimental BPD showed a tendency towards lower levels. CINC1 expression in BALF increased after exposure to hyperoxia for 10 days (13-fold, *P* < 0.001; LPAR1 experiment and 5.0-fold, *P* < 0.01; Ki16425 experiment) and was not

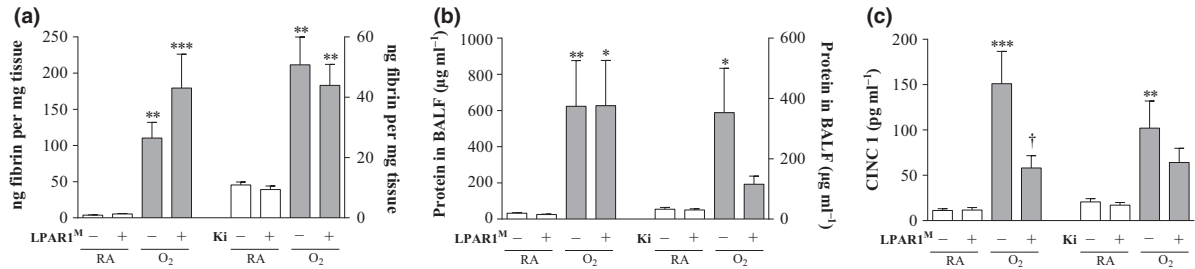


Figure 8 Quantification of extravascular fibrin deposition in lung homogenates (a), and total protein concentration in bronchoalveolar lavage fluid (BALF; b) and CINC1 expression in BALF (c) on day 10 in LPAR1-mutant and wild-type Wistar rat pups. In the LPAR1 experiments pups did not receive treatment. Wild-type pups served as controls in room air (RA) (open bar) and hyperoxia (shaded bar) for LPAR1-mutant rat pups kept in RA (open bar) or hyperoxia (shaded bar). In the Ki16425 experiments, RA pups (open bars) were injected daily with DMSO or Ki16425 and O₂ pups (shaded bars) were injected daily with DMSO or Ki16425: 5 mg kg⁻¹ day⁻¹ until 10 days of age. Values are expressed as mean ± SEM. **P* < 0.05, ***P* < 0.01 and ****P* < 0.001 vs. own RA controls. †*P* < 0.05 vs. age-matched O₂-exposed control. LPAR1^M = LPAR1^{M318R/M318R}-mutant rat; Ki = Ki16425. -: daily administration of solvent (DMSO) in Ki16425 experiments or wild-type rat in LPAR1-mutant rat experiments. +: daily treatment with 5 mg kg⁻¹ of Ki16425 or LPAR1-mutant rat, *n* = 8–12 per group For both experimental models three independent experiments were performed for fibrin deposition, total protein measurement in BALF as a marker for vascular leakage and CINC1 expression in BALF.

affected in rat pups kept under normoxia (Fig. 8c). In LPAR1-deficient rat pups, CINC1 expression decreased 2.6-fold (*P* < 0.05) compared to oxygen-exposed controls. CINC1 expression was not affected significantly after Ki16425 treatment of experimental BPD.

mRNA expression in lung tissue

LPAR1–6 expression during neonatal lung development and experimental BPD. Directly after birth on

neonatal day 1 the mRNA of LPAR1–6 is expressed in the lung (Fig. 9a–f). During early neonatal lung development expression of LPAR2 (b), and LPAR5 (e) and LPAR6 (f) increased, whereas LPAR3 (c) decreased. This resulted in a 2.0-fold (*P* < 0.001), 1.7-fold (*P* < 0.05) and 1.4-fold (*P* < 0.01) increase in mRNA expression for LPAR2, LPAR5 and LPAR6, respectively, on day 10 compared with day 1. During normal lung development LPAR2 expression was increased 1.7-fold (*P* < 0.01) on day 3, and LPAR3 was decreased 1.7-fold (*P* < 0.01) on day 3 and 2.0-

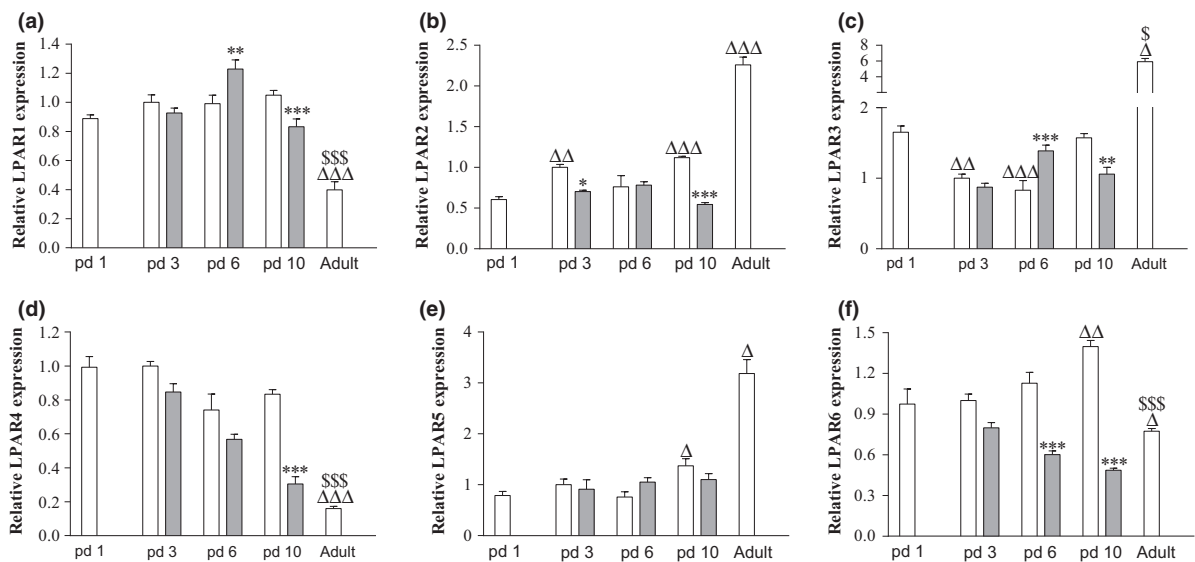


Figure 9 Relative mRNA expression of Lysophosphatidic acid receptor (LPAR) 1 (a), LPAR2 (b), LPAR3 (c), LPAR4 (d), LPAR5 (e) and LPAR 6 (f) in pups on days 1, 3, 6 and 10 after birth (*N* = 12) and in adults (*N* = 5) during normal development (white bars) and after exposure to 100% oxygen (shaded bars). Values are expressed as mean ± SEM. **P* < 0.05, ***P* < 0.01 and ****P* < 0.001 vs. own age-matched room air (RA)-exposed controls. Δ*P* < 0.05, ΔΔ*P* < 0.01 and ΔΔΔ*P* < 0.001 vs. RA control on day 1. §*P* < 0.05 and \$\$\$*P* < 0.001 vs. RA control on day 10.

fold on day 6 ($P < 0.001$) compared with day 1. In adult lung mRNA expression increased 3.6-fold ($P < 0.001$) for LPAR3 compared with day 10 and decreased for LPAR1, LPAR4 (d) and LPAR6 compared with day 10: 2.6-fold ($P < 0.001$) for LPAR1, 5.2-fold ($P < 0.001$) for LPAR4 and 1.8-fold ($P < 0.001$) for LPAR6. Exposure to 100% oxygen for 10 days resulted in a decrease in mRNA expression for LPAR1 (1.3-fold, $P < 0.001$), LPAR2 (2.1-fold, $P < 0.001$), LPAR3 (1.5-fold, $P < 0.01$), LPAR4 (1.5-fold, $P < 0.001$) and LPAR6 (2.9-fold, $P < 0.001$). Exposure to 100% oxygen for 6 days resulted in an increase in mRNA expression for LPAR1 (1.2-fold, $P < 0.01$) and LPAR3 (1.7-fold, $P < 0.001$) and a decrease in expression for LPAR6 (2.9-fold, $P < 0.001$), whereas after 3 days of hyperoxia LPAR2 expression was decreased 1.4-fold ($P < 0.05$) on day 3.

Effects of LPAR1^{M318R} mutation and Ki16425 treatment on mRNA expression in lung tissue. In all rat pups kept under normoxia low levels of mRNA expression (Fig. 10) of the pro-inflammatory factor

chemokine-induced neutrophilic chemoattractant-1 (CINC1; Fig. 10a), the pro-coagulant factor tissue factor (TF; Fig. 10b) and anti-fibrinolytic protein plasminogen activator inhibitor 1 (PAI-1; Fig. 10c), and relatively high levels of mRNA expression of LPAR1 (Fig. 10d), LPAR2 (Fig. 10e) and LPAR3 (Fig. 10f) were observed. Ten days of oxygen exposure resulted in an increase in mRNA expression of CINC-1 (8.3-fold, $P < 0.001$ in LPAR1 control and 11.8-fold, $P < 0.001$ in Ki16425 control), TF (3.0-fold, $P < 0.001$ in LPAR1 control and 2.8-fold, $P < 0.001$ in Ki16425 control) and PAI-1 (40.3-fold, $P < 0.001$ in LPAR1 control and 51.9-fold, $P < 0.001$ in Ki16425 control), and a decrease in mRNA expression of LPAR2 (1.6-fold, $P < 0.01$ in LPAR1 control and $P < 0.001$ in Ki16425 control). Exposure of LPAR1-deficient rat pups to hyperoxia resulted in an increase in mRNA expression of CINC1 (1.8-fold, $P < 0.05$) and a decrease in LPAR1 (1.7-fold, $P < 0.01$; Fig. 10d) and LPAR3 (1.6-fold, $P < 0.05$; Fig. 10f) compared to oxygen-exposed controls. Treatment of oxygen-exposed pups with Ki16425 for 10 days resulted in an increase in mRNA expression

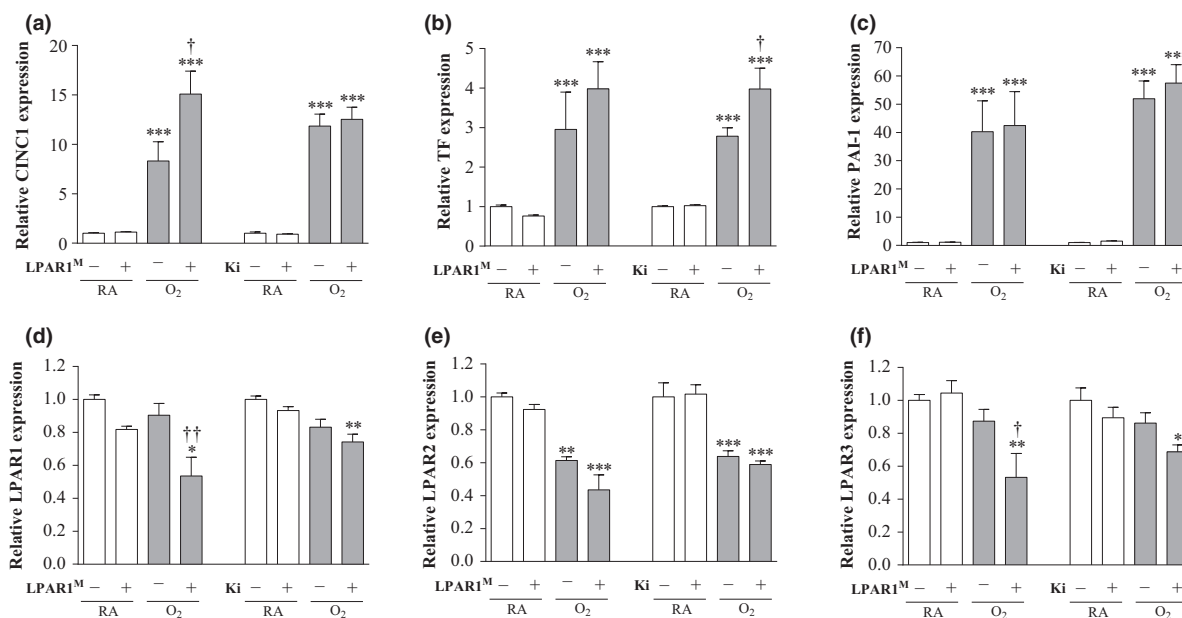


Figure 10 Relative mRNA expression by quantitative real-time RT-PCR in lung homogenates (a–f) of chemokine-induced neutrophilic chemoattractant-1 (CINC1; a), tissue factor (TF; b), plasminogen activator inhibitor 1 (PAI-1; c), LPAR1 (d), LPAR2 (e) and LPAR3 (f) on day 10 in LPAR1-mutant and wild-type Wistar rat pups. Levels of mRNA expression are normalized to that of β -actin. In the LPAR1 experiments pups did not receive treatment. Wild-type pups served as controls in room air (RA) (open bar) and hyperoxia (shaded bar) for LPAR1-deficient rat pups kept in RA (open bar) or hyperoxia (shaded bar). In the Ki16425 experiments, RA pups (open bar) were injected daily with DMSO or Ki16425 (open bars) and O₂ pups (shaded bar) were injected daily with DMSO or Ki16425 (shaded bars): 5 mg kg⁻¹ day⁻¹ until 10 days of age. Values are expressed as mean \pm SEM. * $P < 0.05$, ** $P < 0.01$ and *** $P < 0.001$ vs. own RA controls. † $P < 0.05$ and †† $P < 0.01$ vs. age-matched O₂-exposed controls. LPAR1^M = LPAR1^{M318R/M318R}-mutant rat; Ki = Ki16425. –: daily administration of solvent (DMSO) in Ki16425 experiments or wild-type rat in LPAR1-mutant rat experiments. +: daily treatment with 5 mg kg⁻¹ of Ki16425 or LPAR1-mutant rat, $n = 8$ –10 per group. Three independent experiments were performed for both experimental models.

of TF (1.3-fold, $P < 0.05$) compared to DMSO-treated oxygen-exposed pups.

Effects of LPAR1^{M318R} mutation and Ki16425 treatment on RVH

Because the increase in elastin staining in small arterioles in LPAR1-deficient rats may be associated with vascular remodelling and PAH, and Ki16425 treatment of experimental BPD reduced arteriolar medial wall thickness we investigated RVH on haematoxylin and eosin heart sections (Fig. 11a,b). On neonatal day 10 LPAR1-deficient rat pups developed RVH under normoxia compared to RA Wistar controls, affected by an increase in the ratio RV/LV free wall thickness (1.4-

fold, $P < 0.01$; Fig. 11c), which could be explained by an increase in right ventricular free wall thickness (1.6-fold, $P < 0.001$; Fig. 11a,d). In adult LPAR1-mutant rats the ratio RV/LV free wall thickness was similar to wild-type controls, demonstrating that neonatal RVH in LPAR1-mutant rats is transient. Exposure to hyperoxia for 10 days resulted in an 1.4-fold increase in the ratio RV/LV free wall thickness in Wistar control pups compared to RA controls ($P < 0.05$), but did not aggravate RVH in LPAR1-deficient rat pups compared to LPAR1-deficient controls kept in RA. Administration of Ki16425 for 10 days during normal neonatal development had no adverse effect on the heart (Fig. 11b). Exposure to hyperoxia for 10 days resulted in RVH (Fig. 11b), affected by an 1.3-fold increase in the ratio

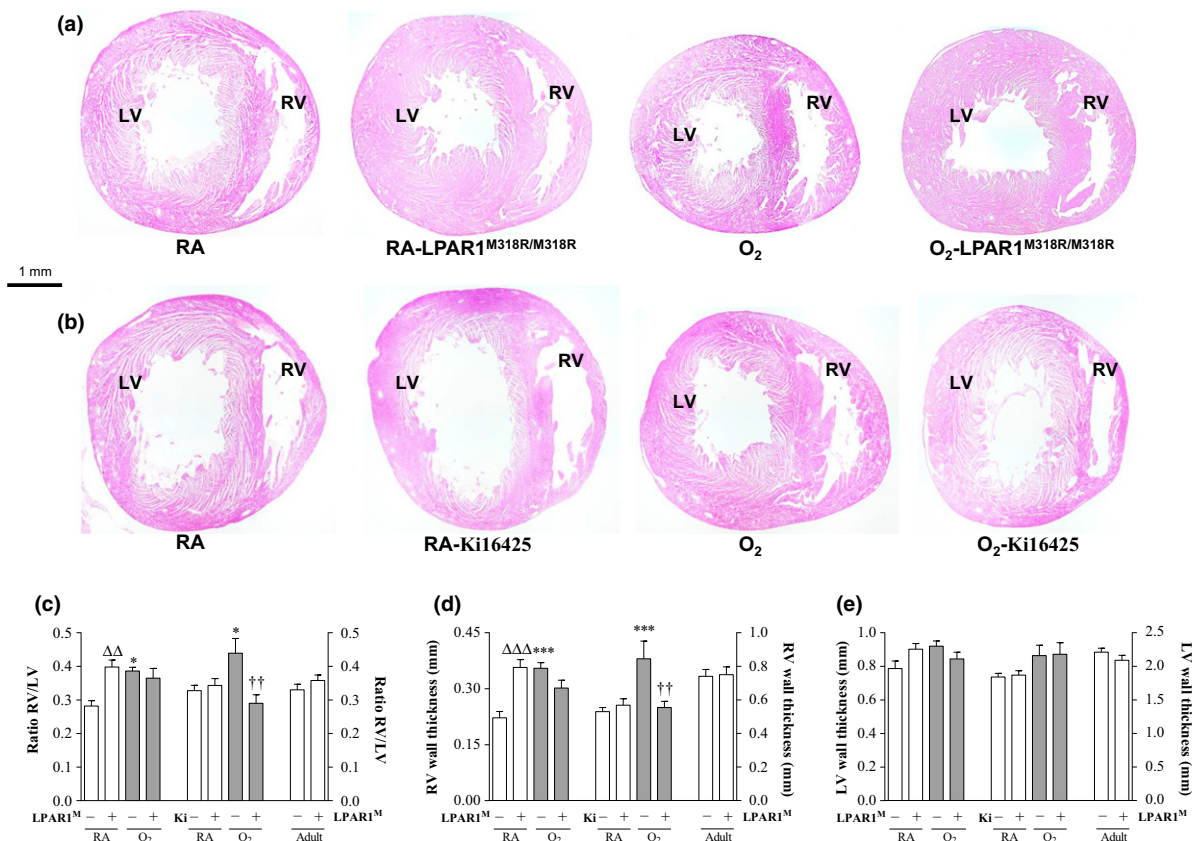


Figure 11 Right ventricular hypertrophy (RVH) was determined in adult rats and in rat pups on day 10 in paraffin sections stained with haematoxylin and eosin (a, b) of LPAR1-mutant and Wistar control rat pups kept in room air (RA) or 100% O₂ (a) and Wistar rat pups kept in RA or 100% O₂ injected daily with 10% DMSO or 5 mg kg⁻¹ day⁻¹ of Ki16425 (b) until 10 days of age. RVH was depicted as RV/LV free wall thickness ratio (c) after measuring RV (d) and LV (e) free wall thickness in RA and age-matched O₂-exposed pups (O₂). Wild-type pups served as controls in RA (open bar) and hyperoxia (shaded bar) for LPAR1-mutant rat pups kept in RA (open bar) or hyperoxia (shaded bar). In the Ki16425 experiments RA pups (open bar) were injected daily with DMSO or Ki16425 and O₂ pups (shaded bar) were injected daily with DMSO or Ki16425: 5 mg kg⁻¹ day⁻¹ until 10 days of age. Data are expressed as mean ± SEM. * $P < 0.05$ and *** $P < 0.001$ vs. own RA controls. ^{ΔΔ} $P < 0.01$ vs. RA Wistar control, ^{††} $P < 0.01$ vs. age-matched O₂-exposed controls. LPAR1^M = LPAR1^{M318R/M318R}-mutant rat; Ki = Ki16425. -: daily administration of solvent (DMSO) in Ki16425 experiments or wild-type rat in LPAR1-mutant rat experiments. +: daily treatment with 5 mg kg⁻¹ of Ki16425 or LPAR1-mutant rat, $n = 8-12$ pups per group and $n = 5$ in adult rats. Three independent experiments were performed for both experimental models.

RV/LV free wall thickness (Fig. 11c) compared to RA controls ($P < 0.05$). Administration of Ki16425 prevented RVH, demonstrated by a normalization in relative RV/LV free wall thickness ($P < 0.01$) compared to oxygen-exposed pups. Hyperoxia and treatment with Ki16425 only effected the right ventricle (Fig. 11d), but not the left ventricle (Fig. 11e). Because transient RVH in LPAR1-deficient rats on day 10, but not in adult rats, cannot be explained by pulmonary hypertension, we investigated whether RVH could be explained by a relatively late closure of the ductus arteriosus. From day 7 onward the ductus arteriosus was rudimentary in both wild-type (Fig. 12a) and LPAR1-mutant rat pups (Fig. 12b). Closure of the ductus arteriosus was demonstrated in haematoxylin- and eosin-stained sections at the level of entrance of the ductus into the aorta in wild-type (Fig. 12c,d) and LPAR1-mutant rat pups on day 7 (Fig. 12e,f). This suggests that neonatal RVH cannot be explained by a relatively late closure of the ductus arteriosus in LPAR1-mutant rats.

Discussion

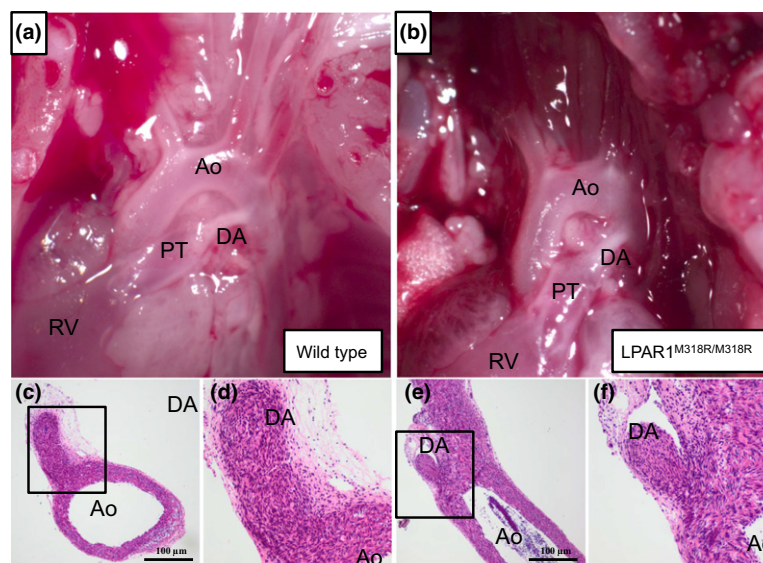
Mutant homozygous LPAR1^{M318R/M318R} rats have an N-ethyl-N-nitrosourea (ENU)-induced missense mutation in helix 8 of LPAR1 that disrupts a highly conserved hydrophobic interaction between the transmembrane 7 domain and helix 8. This causes a reduced and punctate LPAR1 expression at the cell surface, impaired LPA-induced signalling, as shown in primary REFs, an apparent loss-of-function phenotype, which was characterized by a craniofacial disorder (this study and van Boxtel *et al.* 2011), previously observed in LPAR1 knockout mice (Contos *et al.* 2000). In neonatal LPAR1^{M318R/M318R}-mutant rat pups prolonged exposure to hyperoxia, an *in vivo*

model for experimental BPD (Wagenaar *et al.* 2004), survival was prolonged and pulmonary injury was reduced, demonstrated by a decrease in alveolar septal thickness, inflammation and extravascular collagen deposition in the lung. LPAR1 deficiency had no beneficial effects on lung alveolarization, vascularization, arterial medial wall thickness (PAH), capillary-alveolar leakage and fibrin deposition and no adverse effects on normal lung development. Similar beneficial effects on inflammation and extravascular collagen deposition were observed after Ki16425 treatment. In addition, Ki16425 treatment of experimental BPD reduced PAH and prevented RVH, demonstrating that LPAR1 and/or -3 antagonists may be suitable candidates to reduce lung inflammation, fibrosis and PAH-induced RVH in preterm infants with severe BPD.

The receptors LPAR1–6 and autotaxin, the enzyme that is essential for the local production of the ligand LPA, are differentially expressed during lung development and/or in hyperoxia-induced lung injury, suggesting a role for LPA-LPA receptor signalling in the pathophysiology of severe experimental BPD, in which arrested alveolarization, inflammation and pulmonary hypertension play a pivotal role. However, the role of LPA-LPA receptor signalling in experimental BPD is still unclear. The relatively high expression of LPAR1 in the neonatal lung and the adaptive response in mRNA expression in the neonatal lung towards hyperoxia, may contribute to the beneficial pulmonary effects that we observed in LPAR1-deficient rats and after treatment with the LPAR1 and -3 antagonist Ki16425 of rat pups with experimental BPD in this study.

Similar to adult rodents exposure of neonatal rats to hyperoxia for 1 week increases ERK 1/2 phosphorylation in lung tissue homogenates (Lang *et al.* 2010,

Figure 12 Representative pictures of neonatal arterial pole of wild-type (a, c, d) and LPAR1-mutant (b, e, f) rat pups 7 days after birth, showing macroscopically a whitish functionally closed ductus arteriosus (a, b). Microscopically (c, d and e, f) no vascular lumen in the ductus arteriosus could be detected indicating the irreversible process of anatomical closure has occurred in both the WT (c, d) and the LPAR1 mutant (e, f). Boxed areas in panels (c) and (e) are depicted in panels (d) and (f) respectively. Ao, aorta; DA, ductus arteriosus; PT, pulmonary trunk; RV, right ventricle.



Jiang *et al.* 2012, Porzionato *et al.* 2015). When extrapolating our data on reduced ERK 1/2 phosphorylation in embryonic fibroblasts from LPAR1-mutant rats to neonatal lung, we expect reduced LPA-induced ERK 1/2 phosphorylation in neonatal experimental BPD lungs from LPAR1-mutant rats and from rats in which LPAR1 and -3 is pharmacologically blocked compared to oxygen-exposed Wistar control rats. This suggests that reduced ERK activation induced by LPAR1 deficiency or blocking may contribute to the beneficial effects we observed in experimental BPD. Because LPA-induced LPAR1 stimulation and exposure to hyperoxia activate many signal transduction pathways, including ERK and P38 MAPK (Choi *et al.* 2010, Porzionato *et al.* 2015), which may be complicated by redundancy in LPA-LPAR-dependent signalling as demonstrated in the differential expression of LPAR1–6 during normal neonatal lung development and in experimental BPD (Fig. 9), additional experiments are needed to establish the potential beneficial role of reduced LPAR1 and/or -3-induced ERK-phosphorylation in experimental BPD. Differences in response towards hyperoxia-induced neonatal lung injury between the two experimental approaches (LPAR1-mutant rats, deficient in LPAR1 and pharmacological inhibition of LPAR1 and -3) are neutrophil influx and CINC1 expression, RVH and survival. These differences in response towards experimental BPD may be explained by (i) administration of fluid, resulting in a less severe phenotype in the Ki16425 experiments, (ii) potential adverse effects of DMSO (10%) or compound, (iii) a relatively low compound concentration to avoid potential toxic effects of DMSO, (iv) inhibition of both LPAR1 and -3 in the Ki16425 experiments and (v) the continuous absence of LPAR1 during embryonic, foetal and postnatal development in the LPAR1-mutant rats. The absence of a beneficial effect on survival and the influx of neutrophils in the Ki16425 experiments may be explained by the daily administration of fluid. This results in less severe experimental BPD with reduced inflammation (influx of macrophages and neutrophils and CINC1 expression in BALF), vascular leakage, fibrin deposition and mortality in the DMSO-treated control groups, thereby obscuring the potential beneficial effect of Ki16425 on neutrophil influx and survival in experimental BPD, but adverse effects of solvent (10% DMSO) or compound (Ki16425) cannot be excluded. Furthermore, the additional blocking of LPAR3 by Ki16425 and the relatively low concentration of Ki16425 we used in this study with neonatal rats (5 mg kg⁻¹ day⁻¹) compared to adult rodents (up to 20 mg kg⁻¹; Zhao *et al.* 2015) may also contribute to the differences in response between both experimental approaches. The absence of a beneficial effect

on medial wall thickness and RVH in LPAR1-mutant rats may be explained by the development of RVH in LPAR1-mutant rats during neonatal development in RA.

Inflammation is an important contributor to the pathogenesis of BPD, because it may result in severe tissue damage and fibrosis, and treatment with anti-inflammatory agents provides protection against hyperoxia-induced neonatal lung disease or experimental BPD (Yi *et al.* 2004, de Visser *et al.* 2012). LPAR1 deficiency and inhibition protected against hyperoxia-induced neonatal lung injury in rats by reducing fibrosis, as demonstrated by reduced extravascular collagen III deposition, and inflammation, as demonstrated by a reduced pulmonary influx of macrophages and neutrophils in LPAR1-deficient rats, and macrophages after Ki16425 treatment. This resulted in reduced mortality among LPAR1-deficient rats, but not in Ki16425-treated rats. This anti-inflammatory effect was confirmed by the reduction in the neutrophilic attractant CINC1 in BALF in mutant rats, but was not accompanied by the observed expression of the mRNAs of the inflammatory marker CINC1, suggesting the involvement of other chemokines and cytokines, other mechanisms involved in inflammation, including cell adhesion and migration or regulation of gene expression at a post-transcriptional level. Our data are supported by observations in mice deficient in LPAR1 or autotaxin, and mice treated with an LPAR1 antagonist, which are protected against bleomycin-induced fibrosis and mortality (Tager *et al.* 2008, Swaney *et al.* 2010, Oikonomou *et al.* 2012), in allergic asthmatic mice with reduced autotaxin expression or enzymatic activity, which resulted in an attenuated inflammatory response (Park *et al.* 2013) and in Ki16425-treated mice which are protected against LPS-induced peritoneal sepsis (Zhao *et al.* 2015). Pro-inflammatory properties of LPA have been demonstrated in human lung epithelial cells by the secretion of IL8 and activation of NfκB, P38 MAPK and AP1 (Cummings *et al.* 2004, Saatian *et al.* 2006). Blocking of LPAR1 attenuates the LPS-induced proinflammatory response by reducing IL-6 production *in vivo* and *in vitro* in MLE12 mouse lung epithelial cells, probably via inhibition of LPS-induced p38 MAPK phosphorylation and NfκB activation through a direct interaction of CD14 and LPAR1 (Zhao *et al.* 2011).

LPAR1 deficiency in mice is associated with increased perinatal mortality and altered suckling behaviour that may be related to a craniofacial deformation and may lead to a reduction in food intake, bodyweight and survival in the perinatal period (Contos *et al.* 2000). Also LPAR1-mutant rats have a craniofacial deformation (this study and van Boxtel *et al.*

2011), but these rats grow normally, suggesting normal suckling behaviour and milk intake, and are protected against neonatal mortality in hyperoxia compared to Wistar control pups, which may be explained by species specific differences between mice and rats. We only observed increased survival of experimental BPD in LPAR1-deficient rat pups, but not after Ki16425 treatment. This discrepancy in survival between both experiments may be explained by dehydration of LPAR1-deficient rats and their controls or by the lack of selectivity of Ki16425 for LPAR1 and -3. Although we used the same Wistar rat strain as a control, only the pups in the Ki16425 experiments received daily 100 μ L of fluid, thereby reducing potential dehydration and subsequent pathology, as demonstrated by a decreased inflammatory response and mortality in the hyperoxia-exposed control pups in the Ki16425 experiments compared to the control pups with experimental BPD in the LPAR1-deficient rat experiments. The higher survival rate in the oxygen-exposed controls of the Ki16425 experiments may obscure a potential beneficial effect on survival of Ki16425 treatment in experimental BPD. Alternatively, the discrepancy in survival between both experiments may be explained by differences in the efficacy to reduce the pulmonary influx of neutrophilic granulocytes to the lung, which was confirmed by CINC1 expression in BALF, or by a direct effect of aberrant LPAR1 signalling on embryonic development in LPAR1-mutant rats.

LPAR1 deficiency and inhibition did not reduce vascular leakage. This finding is supported by our fibrin deposition data, in which extravascular fibrin deposition depends on leakage of the plasma protein fibrinogen into the alveolar lumen and its local conversion into fibrin by thrombin (Wagenaar *et al.* 2004). These data are in agreement with the absence of a beneficial effect of Ki16425 on LPS-induced protein accumulation in BALF (Zhao *et al.* 2011), but in contrast with beneficial effects of LPAR1 deficiency or pharmacological inhibition of bleomycin-induced vascular leakage in experimental lung fibrosis (Tager *et al.* 2008, Swaney *et al.* 2010). These differences in the efficacy to reduce pulmonary vascular leakage may be explained, at least in part, by differences in animal models, species, receptor antagonist and the onset and progression of tissue damage in these models of experimental lung disease.

A role for LPA in the cardiovascular system is demonstrated in atherosclerosis (Schober & Siess 2012) and the regulation of blood pressure *in vivo*, both as a vasopressor and a vasodilator depending on the species studied and experimental setup (Tokumura *et al.* 1978, 1995). In mice, LPA is a potent endothelial nitric oxide synthase-dependent vasodilator of the intact thoracic aorta (Ruisanchez *et al.* 2014). This

LPA-induced vasodilation response of intact thoracic aortas is LPAR1-dependent, because it can be abolished by pharmacological inhibition of LPAR1 (Ruisanchez *et al.* 2014). On the basis of these experimental data, we expected an adverse effect of LPAR1 blocking or deficiency on PAH. However, LPAR1 and -3 blocking reduced medial wall thickness of small arterioles, which was confirmed by a reduction in RVH, whereas LPAR1 deficiency had no beneficial effect on PAH, thereby confirming the data observed in LPAR1 knockout mice (Cheng *et al.* 2012). The discrepancy in response towards PAH-induced RVH in LPAR1-mutant and Ki16425-treated rat pups with BPD may be explained by: (i) a direct effect of aberrant LPAR1 signalling on embryonic lung and heart development in LPAR1-mutant rats only, resulting in neonatal RVH or (ii) a beneficial effect of LPAR1 and -3 inhibition on PAH in Ki16425-treated rat pups. LPAR1 and -2 double knockout mice suffered from lung vascular remodelling and RVH (Cheng *et al.* 2012). Interestingly, we observed an increase in elastin expression in small arterioles in LPAR1-deficient rats, which was not associated with an increase in our marker for PAH, i.e. increased medial wall thickness, but was associated with RVH. LPAR1 has a wide spread tissue distribution and is expressed in many cell types, including endothelial and (vascular) smooth muscle cells in blood vessels. We speculate that LPA-induced LPAR1 activation on the endothelium may lead to vasodilation, whereas LPAR1 activation on vascular smooth muscle cells may lead to vasoconstriction (Ruisanchez *et al.* 2014). In the cardiovascular system this behaviour is also observed for other receptors, including the apelin receptor APJ, bradykinin B1 and B2 receptors and muscarinic receptors, and may be complicated by receptor expression on inflammatory cells and cardiomyocytes (Obi *et al.* 1994, Felipe *et al.* 2007, Japp & Newby 2008). Because we observed transient RVH in LPAR1-deficient rats on day 10, but not in adult rats, which cannot be explained by pulmonary hypertension, we investigated whether RVH could be explained by a delayed adaptation of the foetal circulation directly after birth by studying relatively late closure of the ductus arteriosus. The ductus arteriosus was closed in both wild-type and LPAR1-mutant rat pups from day 7 onward. Therefore, it remains unlikely that a delayed closure of the ductus arteriosus contributes to neonatal RVH and may be explained by other developmental differences in foetal and early neonatal heart development, including a persisting foramen ovale in LPAR1-mutant neonatal rats, for which additional research is needed. In addition, no right ventricular outflow obstructions or ventricular septal defects were observed in neonatal and adult

hearts that could explain the transient RVH in LPAR1-mutant rats.

When the absence of adverse effects of treatment with LPAR1 and/or -3 blockers in rats is confirmed in patients, extrapolation of the beneficial effects of LPAR1 deficiency and treatment with blockers of LPAR1 or LPAR1 and -3 in rat pups with experimental BPD to preterm infants with respiratory failure, may result in a beneficial effect on lung inflammation, PAH and fibrosis which are major reasons for mortality or morbidity in preterm infants with severe BPD.

Conflict of interest

The authors report no conflicts of interest to disclose.

The authors gratefully acknowledge Mrs. I. van Ark and Mrs. T.A. Leusink-Muis (Department of Pharmacology, Utrecht University, Utrecht, the Netherlands), and Mrs C. van Munsteren (Department of Anatomy and Embryology, Leiden University Medical Center, Leiden, the Netherlands) for expert technical assistance, Dr. E. de Heer (Department of Pathology, Leiden University Medical Center, Leiden, the Netherlands) for providing the ED-1 antibody and Dr. J.J. Baelde (Department of Pathology, Leiden University Medical Center, Leiden, the Netherlands) for providing the COL3A antibody. This work was supported by the National Institutes of Health (grants 1R01 HL092158 and 1R01 ES015330; FW); a grant from the China Scholarship Council (XC) and grants from the Stichting Zeldzame Ziekten Fonds, Gisela Thier Foundation and Chiesi Pharmaceuticals BV (GW and FW).

Author contributions

F.W., E.C., G.F. and G.W. participated in research design. X.C., E.L., R.S., R.B. and G.W. conducted experiments. X.C., E.L., R.S., R.B., M.D. and G.W. performed data analysis. X.C., F.W., R.B., E.C., G.F. M.D. and G.W. wrote or contributed to the writing of the manuscript.

References

Abman, S.H. 2009. Role of endothelin receptor antagonists in the treatment of pulmonary arterial hypertension. *Annu Rev Med* 60, 13–23.

Baraldi, E. & Filippone, M. 2007. Chronic lung disease after premature birth. *N Engl J Med* 357, 1946–1955.

van Boxtel, R., Gould, M.N., Cuppen, E. & Smits, B.M. 2010. ENU mutagenesis to generate genetically modified rat models. *Methods Mol Biol* 597, 151–167.

van Boxtel, R., Vroiling, B., Toonen, P., Nijman, I.J., van Roekel, H., Verheul, M., Baakman, C., Guryev, V., Vriend, G. & Cuppen, E. 2011. Systematic generation of in vivo G protein-coupled receptor mutants in the rat. *Pharmacogenomics J* 11, 326–336.

Cheng, H.Y., Dong, A., Panchatcharam, M., Mueller, P., Yang, F., Li, Z., Mills, G., Chun, J., Morris, A.J. &

Smyth, S.S. 2012. Lysophosphatidic acid signaling protects pulmonary vasculature from hypoxia-induced remodeling. *Arterioscler Thromb Vasc Biol* 32, 24–32.

Choi, J.W., Herr, D.R., Noguchi, K., Yung, Y.C., Lee, C.W., Mutoh, T., Lin, M.E., Teo, S.T., Park, K.E., Mosley, A.N. & Chun, J. 2010. LPA receptors: subtypes and biological actions. *Annu Rev Pharmacol Toxicol* 50, 157–186.

Contos, J.J., Fukushima, N., Weiner, J.A., Kaushal, D. & Chun, J. 2000. Requirement for the lpA1 lysophosphatidic acid receptor gene in normal suckling behavior. *Proc Natl Acad Sci USA* 97, 13384–13389.

Cummings, R., Zhao, Y., Jacoby, D., Spannhake, E.W., Ohba, M., Garcia, J.G., Watkins, T., He, D., Saatian, B. & Natarajan, V. 2004. Protein kinase Cdelta mediates lysophosphatidic acid-induced NF-kappaB activation and interleukin-8 secretion in human bronchial epithelial cells. *J Biol Chem* 279, 41085–41094.

Felipe, S.A., Rodrigues, E.S., Martin, R.P., Paiva, A.C., Pesquero, J.B. & Shimuta, S.I. 2007. Functional expression of kinin B1 and B2 receptors in mouse abdominal aorta. *Braz J Med Biol Res* 40, 649–655.

Gehret, A.U., Jones, B.W., Tran, P.N., Cook, L.B., Greuber, E.K. & Hinkle, P.M. 2010. Role of helix 8 of the thyrotropin-releasing hormone receptor in phosphorylation by G protein-coupled receptor kinase. *Mol Pharmacol* 77, 288–297.

Japp, A.G. & Newby, D.E. 2008. The apelin-APJ system in heart failure: pathophysiologic relevance and therapeutic potential. *Biochem Pharmacol* 75, 1882–1892.

Jiang, J.S., Lang, Y.D., Chou, H.C., Shih, C.M., Wu, M.Y., Chen, C.M. & Wang, L.F. 2012. Activation of the renin-angiotensin system in hyperoxia-induced lung fibrosis in neonatal rats. *Neonatology* 101, 47–54.

Jobe, A.H. 1999. The new BPD: an arrest of lung development. *Pediatr Res* 46, 641–643.

Lang, Y.D., Hung, C.L., Wu, T.Y., Wang, L.F. & Chen, C.M. 2010. The renin-angiotensin system mediates hyperoxia-induced collagen production in human lung fibroblasts. *Free Radic Biol Med* 49, 88–95.

Lin, M.E., Herr, D.R. & Chun, J. 2010. Lysophosphatidic acid (LPA) receptors: signaling properties and disease relevance. *Prostaglandins Other Lipid Mediat* 91, 130–138.

Moolenaar, W.H., van Meeteren, L.A. & Giepmans, B.N. 2004. The ins and outs of lysophosphatidic acid signaling. *BioEssays* 26, 870–881.

Obi, T., Kabeyama, A. & Nishio, A. 1994. Characterization of muscarinic receptor subtype mediating contraction and relaxation in equine coronary artery in vitro. *J Vet Pharmacol Ther* 17, 226–231.

Oikonomou, N., Mouratis, M.A., Tzouveleki, A., Kaffe, E., Valavanis, C., Vilaras, G., Karameris, A., Prestwich, G.D., Bouros, D. & Aidinis, V. 2012. Pulmonary autotaxin expression contributes to the pathogenesis of pulmonary fibrosis. *Am J Respir Cell Mol Biol* 47, 566–574.

Park, G.Y., Lee, Y.G., Berdyshev, E., Nyenhuis, S., Du, J., Fu, P., Gorshkova, I.A., Li, Y., Chung, S., Karpurapu, M. et al. 2013. Autotaxin production of lysophosphatidic acid mediates allergic asthmatic inflammation. *Am J Respir Crit Care Med* 188, 928–940.

- Porzionato, A., Sfriso, M.M., Mazzatenta, A., Macchi, V., De Caro, R. & Di Giulio, C. 2015. Effects of hyperoxic exposure on signal transduction pathways in the lung. *Respir Physiol Neurobiol* 209, 106–114.
- Pyne, N.J., Dubois, G. & Pyne, S. 2013. Role of sphingosine 1-phosphate and lysophosphatidic acid in fibrosis. *Biochim Biophys Acta* 1831, 228–238.
- Rancoule, C., Pradère, J.P., Gonzalez, J., Klein, J., Valet, P., Bascands, J.L., Schanstra, J.P. & Saulnier-Blache, J.S. 2011. Lysophosphatidic acid-1-receptor targeting agents for fibrosis. *Expert Opin Investig Drugs* 20, 657–667.
- Ruisanchez, É., Dancs, P., Kerék, M., Németh, T., Faragó, B., Balogh, A., Patil, R., Jennings, B.L., Liliom, K., Malik, K.U., Smrcka, A.V., Tigyi, G. & Benyó, Z. 2014. Lysophosphatidic acid induces vasodilation mediated by LPA1 receptors, phospholipase C, and endothelial nitric oxide synthase. *FASEB J* 28, 880–890.
- Saatian, B., Zhao, Y., He, D., Georas, S.N., Watkins, T., Spannhake, E.W. & Natarajan, V. 2006. Transcriptional regulation of lysophosphatidic acid-induced interleukin-8 expression and secretion by p38 MAPK and JNK in human bronchial epithelial cells. *Biochem J* 393, 657–668.
- Schober, A. & Siess, W. 2012. Lysophosphatidic acid in atherosclerotic diseases. *Br J Pharmacol* 167, 465–482.
- Shea, B.S. & Tager, A.M. 2012. Role of the lysophospholipid mediators lysophosphatidic acid and sphingosine 1-phosphate in lung fibrosis. *Proc Am Thorac Soc* 9, 102–110.
- Simon, D.M., Tsai, L.W., Ingenito, E.P., Starcher, B.C. & Mariani, T.J. 2010. PPARgamma deficiency results in reduced lung elastic recoil and abnormalities in airspace distribution. *Respir Res* 11, 69.
- Steinhorn, R.H. 2010. Neonatal pulmonary hypertension. *Pediatr Crit Care Med* 11, S79–S84.
- Stortelers, C., Kerkhoven, R. & Moolenaar, W.H. 2008. Multiple actions of lysophosphatidic acid on fibroblasts revealed by transcriptional profiling. *BMC Genom* 9, 387.
- Swaney, J.S., Chapman, C., Correa, L.D., Stebbins, K.J., Bundy, R.A., Prodanovich, P.C., Fagan, P., Baccei, C.S., Santini, A.M., Hutchinson, J.H., Seiders, T.J., Parr, T.A., Prasit, P., Evans, J.F. & Lorrain, D.S. 2010. A novel, orally active LPA(1) receptor antagonist inhibits lung fibrosis in the mouse bleomycin model. *Br J Pharmacol* 160, 1699–1713.
- Tager, A.M., LaCamera, P., Shea, B.S., Campanella, G.S., Selman, M., Zhao, Z., Polosukhin, V., Wain, J., Karimi-Shah, B.A., Kim, N.D. et al. 2008. The lysophosphatidic acid receptor LPA1 links pulmonary fibrosis to lung injury by mediating fibroblast recruitment and vascular leak. *Nat Med* 14, 45–54.
- Toews, M.L., Ediger, T.L., Romberger, D.J. & Rennard, S.I. 2002. Lysophosphatidic acid in airway function and disease. *Biochim Biophys Acta* 1582, 240–250.
- Tokumura, A., Fukuzawa, K. & Tsukatani, H. 1978. Effects of synthetic and natural lysophosphatidic acids on the arterial blood pressure of different animal species. *Lipids* 13, 572–574.
- Tokumura, A., Yotsumoto, T., Masuda, Y. & Tanaka, S. 1995. Vasopressor effect of lysophosphatidic acid on spontaneously hypertensive rats and Wistar Kyoto rats. *Res Commun Mol Pathol Pharmacol* 90, 96–102.
- Tuder, R.M., Abman, S.H., Braun, T., Capron, F., Stevens, T., Thistlethwaite, P.A. & Haworth, S.G. 2009. Development and pathology of pulmonary hypertension. *J Am Coll Cardiol* 54, S3–S9.
- de Visser, Y.P., Walther, F.J., Laghmani, E.H., Boersma, H., van der Laarse, A. & Wagenaar, G.T.M. 2009. Sildenafil attenuates pulmonary inflammation and fibrin deposition, mortality and right ventricular hypertrophy in neonatal hyperoxic lung injury. *Respir Res* 10, 30.
- de Visser, Y.P., Walther, F.J., Laghmani, E.H., van der Laarse, A. & Wagenaar, G.T.M. 2010. Apelin attenuates hyperoxic lung and heart injury in neonatal rats. *Am J Respir Crit Care Med* 182, 1239–1250.
- de Visser, Y.P., Walther, F.J., Laghmani, E.H., Steendijk, P., Middeldorp, M., van der Laarse, A. & Wagenaar, G.T.M. 2012. Phosphodiesterase-4 inhibition attenuates persistent heart and lung injury by neonatal hyperoxia in rats. *Am J Physiol Lung Cell Mol Physiol* 302, L56–L67.
- Wagenaar, G.T.M., ter Horst, S.A., van Gastelen, M.A., Leijser, L.M., Mauad, T., van der Velden, P.A., de Heer, E., Hiemstra, P.S., Poorthuis, B.J. & Walther, F.J. 2004. Gene expression profile and histopathology of experimental bronchopulmonary dysplasia induced by prolonged oxidative stress. *Free Radic Biol Med* 36, 782–801.
- Wagenaar, G.T.M., Laghmani, E.H., de Visser, Y.P., Sengers, R.M., Steendijk, P., Baelde, H.J. & Walther, F.J. 2013. Ambrisentan reduces pulmonary arterial hypertension, but does not stimulate alveolar and vascular development in neonatal rats with hyperoxic lung injury. *Am J Physiol Lung Cell Mol Physiol* 304, L264–L275.
- Yi, M., Jankov, R.P., Belcastro, R., Humes, D., Copland, I., Shek, S., Swezey, N.B., Post, M., Albertine, K.H., Auten, R.L. & Tanswell, A.K. 2004. Opposing effects of 60% oxygen and neutrophil influx on alveologenesis in the neonatal rat. *Am J Respir Crit Care Med* 170, 1188–1196.
- Zhao, Y. & Natarajan, V. 2013. Lysophosphatidic acid (LPA) and its receptors: role in airway inflammation and remodeling. *Biochim Biophys Acta* 1831, 86–92.
- Zhao, J., He, D., Su, Y., Berdyshev, E., Chun, J., Natarajan, V. & Zhao, Y. 2011. Lysophosphatidic acid receptor 1 modulates lipopolysaccharide-induced inflammation in alveolar epithelial cells and murine lungs. *Am J Physiol Lung Cell Mol Physiol* 301, L547–L556.
- Zhao, J., Wei, J., Weathington, N., Jacko, A.M., Huang, H., Tsung, A. & Zhao, Y. 2015. Lysophosphatidic acid receptor 1 antagonist ki16425 blunts abdominal and systemic inflammation in a mouse model of peritoneal sepsis. *Transl Res* 166, 80–88.

Supporting Information

Additional Supporting Information may be found in the online version of this article:

Figure S1. Transfection efficiency is similar between wild-type and mutant LPAR1 expressing plasmids.